Master Thesis

Genetic engineering of *Aureobasidium pullulans* based on the gene *ura3* and the role of Dia3 in the biosynthetic pathway of diaporthinic acid in *Trichoderma reesei*

carried out for the purpose of obtaining the degree of
Master of Science, submitted at TU Wien,
Faculty of Technical Chemistry, by

Univ.-Prof. Mag. Dr.rer.nat. Robert Mach
and
Senior Scientist Mag.rer.nat. Dr.rer.nat. Christian Zimmermann

E166 - Institute of Chemical, Environmental and Bioscience Engineering

submitted to the TU Wien
Faculty of Technical Chemistry

by

Polina Atanasova
[redacted]

Vienna, September 16, 2025

Affidavit

I confirm, that going to press of this thesis with the title

Genetic engineering of *Aureobasidium pullulans* based on the gene *ura3* and the role of Dia3 in the biosynthetic pathway of diaporthinic acid in *Trichoderma reesei*

needs the confirmation of the examination committee. I declare in lieu of oath, that I wrote this thesis and carried out the associated research myself, using only the literature cited in this volume. If text passages from sources are used literally, they are marked as such. I confirm that this work is original and has not been submitted for examination elsewhere, nor is it currently under consideration for a thesis elsewhere. I acknowledge that the submitted work will be checked electronically-technically using suitable and state-of-the-art means (plagiarism detection software). On the one hand, this ensures that the submitted work was prepared according to the high-quality standards within the applicable rules to ensure good scientific practice "Code of Conduct" at the TU Wien. On the other hand, a comparison with other student theses avoids violations of my personal copyright.

Vienna, September 16, 2025

Signature

Vienna, September 16, 2025

Contents

September 16, 2025

Abbreviations

5-FOA	5-Fluoroorotic Acid
CRISPR	Clustered Regularly Interspaced Short Palindromic Repeats
DTT	Dithiothreitol
LB	Lysogeny Broth
MAM	Mandels Andreotti Medium
MEX	Malt Extract Medium
OMP	Orotidine 5-Monophosphate
PCR	Polymerase Chain Reaction
PEG	Polyethylene Glycol
ROS	Reactive Oxygen Species
RT	Room Temperature
RT-qPCR	Reverse Transcription Quantitative Polymerase Chain Reaction
UMP	Uridine Monophosphate
YPD	Yeast extract Peptone Dextrose

September 16, 2025

PROJECT A

Genetic engineering of *Aureobasidium pullulans* based on the gene *ura3*: opportunities and challanges

Abstract

The yeast-like genus *Aureobasidium* is a polymorphic, multi-budding, ubiquitous fungus often encountered in various locations. The organism is characterized by morphological plasticity and the ability to thrive in oligotrophic environments, adapting to unique and atypical habitats. Industrially, *A. pullulans* is highly significant, since most strains are able to produce the extracellular polysaccharide pullulan.

The aim of this work was to obtain a deletion strain of *A. pullulans* EXF-150, with the further perspective of achieving a simple molecular tool for the genetic manipulation of the yeast-like fungus. Therefore the gene *ura3* was targeted, encoding for orotidine 5'-phosphate decarboxylase. An active gene results in the expression of orotidine 5'-phosphate 4-decarboxylase, catalyzing the decarboxylation of Orotidine 5-Monophosphate (OMP) to Uridine Monophosphate (UMP). When 5-Fluoroorotic Acid (5-FOA) is added to the selection medium, the enzyme converts 5-FOA to 5-fluorouracil, inevitably leading to cell death. On the contrary, a successful deletion of the gene, 5-FOA cannot be converted to 5-fluorouracil, resulting in viable cells.

Intended deletion of the gene *ura3* via protoplast-mediated and chemical transformation resulted in an induced missense mutation, whereby a nucleic acid base substitution (C to A), leads to an amino acid substitution (cysteine to alanine). The generated deletion strains were capable of growing on selction medium containg 5-FOA. This outcome is suspected to be connected to protein loss of function, due to the amino acid substitution. Furthermore, it can be assumed that the mutation is induced by Cas9 activity, since it occurs in close proximity to the intented cut site of Cas9. This again can occur as a consequence of inaccurate DNA repair mechanisms.

The study emphasizes reoccuring problems of different transformation methods and shows how these can pose as a stress factor for the organisms, forcing them to adapt to unfavourable habitats.

Kurzfassung

Aureobasidium ist ein polymorpher und ubiquitärer Pilz, der sich durch seine morphologische Plastizität und die Fähigkeit auszeichnet, in oligotrophen Umgebungen zu wachsen und sich an atypische Lebensräume anzupassen. Industriell ist *A. pullulans* sehr signifikant, da die meisten Stämme das extrazelluläre Polysaccharid Pullulan produzieren können.

Das Ziel dieser Arbeit war es, einen Deletionsstamm von *A. pullulans* EXF-150 zu generieren, mit der weiteren Perspektive, ein simples molekulares Werkzeug für die genetische Manipulation des Pilzes zu entwickeln. Für die Deletion wurde das Gen *ura3* gewählt, das für Orotidin-5'-phosphat-Decarboxylase kodiert. Ein aktives Gen führt zur Expression von Orotidin-5'-phosphat-4-decarboxylase, welche die Decarboxylierung von Orotidine 5-Monophosphate (OMP) zu Uridine Monophosphate (UMP) katalysiert. Durch Zugabe von 5-Fluoroorotic Acid (5-FOA) zum Selektionsmedium, wandelt das Enzym 5-FOA in 5-Fluorouracil um, was zwangsläufig zum Zelltod führt. Im Gegensatz dazu kann bei einer erfolgreichen Deletion des Gens 5-FOA nicht in 5-Fluoruracil umgewandelt werden, was wiederum zu lebensfähigen Zellen führt.

Die angestrebte Deletion des Gens *ura3* durch Protoplasten vermittelte und chemische Transformation führte zu einer Missense-Mutation, bei der eine Nukleinsäurebasensubstitution (C zu A) zu einer Aminosäuresubstitution (Cystein zu Alanin) führt. Durch die induzierte Substitution konnten die Stämme in weiterer Folge auf das Selektionsmedium wachsen. Dieses Ergebnis ist möglicherweise auf einen Funktionsverlust des Proteins aufgrund der Aminosäuresubstitution zurückzuführen. Darüber hinaus kann angenommen werden, dass die Mutation durch die Cas9-Aktivität induziert wird, da sie in unmittelbarer Nähe der angestrebten Schnittstelle von Cas9 auftritt. Dies kann wiederum eine Konsequenz ungenauer DNA-Reparaturmechanismen sein.

Diese Arbeit unterstreicht wiederkehrende Probleme verschiedener Transformationsmethoden und zeigt, wie diese einen Stressfaktor für die Organismen darstellen können, der sie wiederum dazu zwingt, sich an unvorteilhafte Lebensräume anzupassen.

September 16, 2025

1. Introduction

The yeast-like organism *Aureobasidium* is a polymorphic, multi-budding, ubiquitous fungus belonging to the family of *Dothideaceae*, order *Dothideales*. So far, approximately 40 *Aureobasidium* species have been officially described [1], whereby classification is mainly based on morphology and phylogeny. Historically, *Aureobasidium* was first described in 1866 by De Bary [2] under the name *Dematium pullulans*. However, the genus itself was introduced by Viala & Boyer in 1891 in connection to the scalding of grape plants [2].

Aureobasidium pullulans is an ubiquitous organism, often encountered in locations characterized by extreme and harsh environmental conditions, such as space [3] and hypersaline waters [4], indicating the organism's resilience to stress and high salt concentrations. Various *Aureobasidium* species were found in regions with fluctuating temperatures, such as Antarctica and Egypt, but also in tropical areas with high humidity, such as Thailand and India [5][6][7]. Indoors, *A. pullulans* was isolated from wet environments, such as refrigerators and kitchen utilities [8]. Furthermore, the yeast-like fungus was successfully isolated from the surface of grapes and apples, as well as from the roots of plants, such as the highland rush (*Juncus trifidus*) [8]. One of the rather extraordinary isolation locations of *A. pullulans* was the surface of a fourth block wall of the highly radioactive Chornobyl [9]. The reference strain *A. pullulans* EXF-150 was first isolated from a hypersaline environment with a salinity concentration between 3 - 30% [4]. The variety in habitats is mirrored in the morphological plasticity of the organism and its ability to thrive in oligotrophic environments and to adapt to unique and atypical habitats.

Morphological plasticity is often associated with the survival and adaptation of fungi to different environmental conditions. Thus, the morphology and phenotype of *Aureobasidium* strains vary depending on their natural habitat [10] and can be influenced by the chosen carbon source, incubation time, temperature, and provided substrate [11]. Typical *A. pullulans* colonies are in the color range of creamy white, slightly pinkish or pale brown, and, depending on growing conditions and age, can turn black [3]. The black pigmentation is associated with melanin production (therefore, *Aureobasidium* is often referred to as black-yeast fungi) [2][3][12]. Fungi are known for their universal utilization of melanin, a black pigment mainly contained within

the cell wall. Melanin serves as an adaptation technique and contributes to persistence under stress. It plays a crucial role in radiation protection, confers virulence, and supports the immune system's defense response [12].

Throughout literature, *Aureobasidium* is described either as a dimorphic [13] or polymorphic [14] organism; however, when referring to it as a dimorphic organism, differentiation is based solely on yeast-like and mycelial morphology. The organism's complexity and morphological plasticity often lead to confusion regarding its life cycle. The suggested life cycle starts with the formation of blastoconidia (Figure 1.1,A)), yeast-like cells essential for asexual reproduction, further developing into pseudo-mycelium or swollen cells (septated or not-septated) [11][15]. The pseudo-mycelium can then either grow to branched hyphae with buddings, releasing blastoconidia that can later form chlamydospores, or to (aerial) hyphae, which are able to produce chlamydospores divided by septa. Hence, each section acts as an individual cell that produces blastoconidia [11][15]. Swollen cells produce blastoconidia, further resulting in chlamydospores, or yield into mycelium with septa.

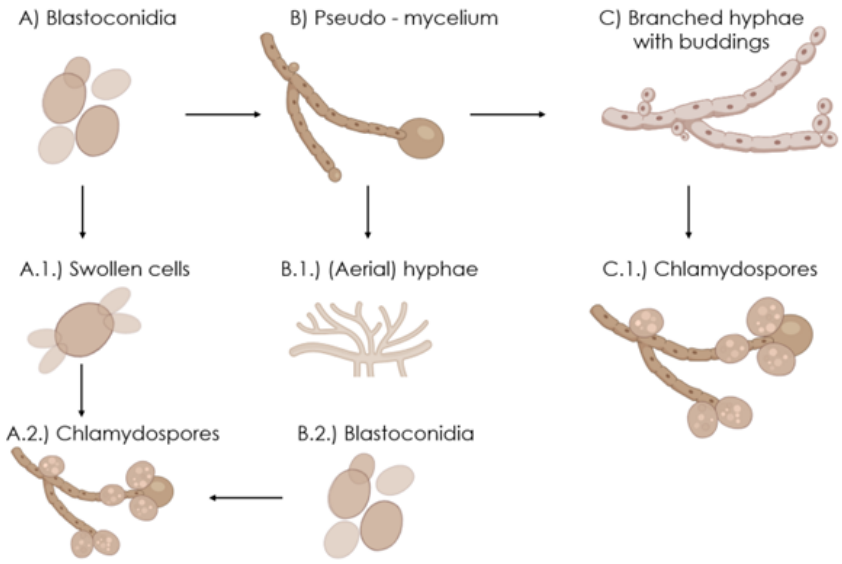

Figure 1.1.: The proposed life cycle of *Aureobasidium pullulans*, however throughout literature the life cycle can vary depending on classification method

Industrially, *A. pullulans* is highly significant since most strains can produce the extracellular polysaccharide pullulan, widely used as wrapping and coating material, because of its biodegradability [3][5]. In the food industry, it serves for the production of food additives and

different medical supplements, such as β-glucan, a supplement often added as an immune system booster and antihypertensive, produced by *Aureobasidium pullulans* NP1221. Another example of a vital food supplement produced by *Aureobasidium sp.* SN-124A is erythritol, commonly used as an artificial sweetener. Many *Aureobasidium strains* are capable of producing a plethora of industrially essential enzymes, such as lipase, sucrase, and β-galactosidase, typically used in the dairy industry [3]. In addition, *A. pullulans* is widely used for its antagonistic properties against pathogens as a natural biocontrol agent [5].

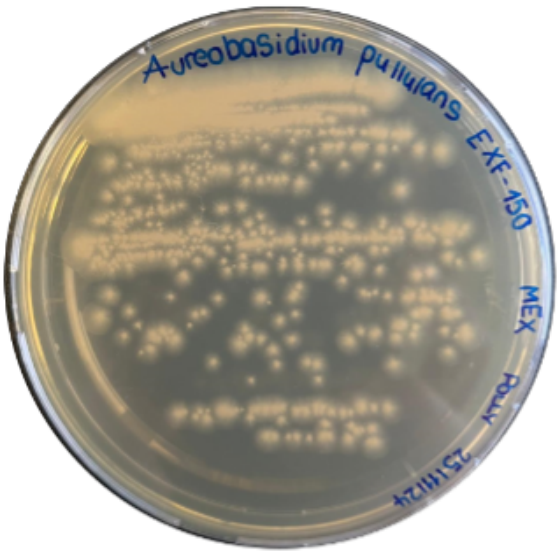

Figure 1.2.: *Aureobasidium pullulans* EXF-150 on MEX (after 72 h of incubation at 24 °C); visible creamy white colonies

1.1. The significance of *Aureobasidium pullulans* in biotechnology

In biotechnology, fungi have gained great significance over time due to their ability to produce secondary metabolites, whose application fields cover medicine, food industry, agriculture, and many more [16].

The progress in genetic transformation techniques facilitated the targeted genetic modification of fungi. Thereby the insertion or deletion of genetic information, such as promotor regions or

transcription factors, consequently allowing or improving the expression of endogenous genes was enabled [17]. Although there are established transformation protocols for many fungi, difficulties often occur. Protoplast-mediated transformation (PTM), Agrobacterium-mediated method, biolistic transformation, or electroporation belong to the standardized techniques for fungal transformation [17]. However, each strain requires an individual optimization of the applied transformation method.

Studies report a successful transformation of *A. pullulans* through protoplast-mediated transformation [18] and chemical transformation [14]. Protoplast-mediated transformation starts with the preparation of protoplasts, using an enzyme solution that targets different chemical bonds in the fungal cell wall and breaks them, in order to make the cell wall more accessible for the exogenous DNA. Since protoplasts are extremely fragile, stabilizers, such as sorbitol (usually between 0.8 and 1.2 M), are added to the buffers. The main purpose of adding sorbitol to the media, is to reduce the osmotic stress and thereby increase cell viability [19]. Furthermore, supplementation of the buffers with calcium and PEG is necessary to increases DNA uptake.

Prior the exposition of cells to selection medium, they are left to recover in order to restore normal function, repair disrupted cell walls, and adapt. Simplicity and the fact that there are no requirements for expensive tools are some of the advantages of this technique. However, protoplast mediated transformation is also accompanied by some disadvantages. One of the challenges is the composition of the fungal cell wall, which mainly consists of chitin and glucan, but can differ highly between strains; hence, the enzyme solution requires optimization for each strain individually. In addition, the process is time-consuming, transformants are often obtained after 1-3 weeks, and buffers have to be previously adapted [18].

Chemical transformation requires treatment of the cells with a chemical solution, often including calcium, however for *A. pullulans*, the solution is a combination of Tris, EDTA, and sorbitol. Consequently, carrier DNA and linear DNA are added for transformation, followed by a recovery of the cells and, finally, exposition to a selection medium. Chemical transformation often requires the know-how and experience since most steps should be performed rapidly and on ice. Competent cells must be treated carefully due to the chemical treatment, hence the fragile cell wall. Transformants are obtained in 3-4 days, which makes this technique faster than PTM.

1.2. *ura3* – Orotidine 5-phosphate decarboxylase

In the scope of this work the gene *ura3* was targeted. *Ura3* encodes for orotidine 5'-phosphate decarboxylase, which is commonly applied as a selection method for genetic modifications in yeast. An active gene results in the expression of orotidine 5'-phosphate decarboxylase, which catalyzes a reaction in the de novo biosynthesis of pyrimidine [20], more precisely, the decarboxylation of orotidine 5-monophosphate (OMP) to uridylic acid (UMP) [21][22]. When 5-fluoroorotic acid (5-FOA) is added to the selection medium, the enzyme converts 5-FOA to 5-fluorouracil, which acts as a cytotoxic substance, inevitably leading to cell death [23] [24][25]. On the contrary, if the gene is successfully deleted, 5-FOA cannot be converted to 5-fluorouracil, resulting in viable cells.

By deleting *ura3*, the selection media must be supplemented with uridine, since a successful deletion leads to a loss of uridine prototrophy [25]. Positive transformants will not be viable on media without uridine supplementation. A schematic visualization (Figure 1.3) summarizes the function principle of the selection method.

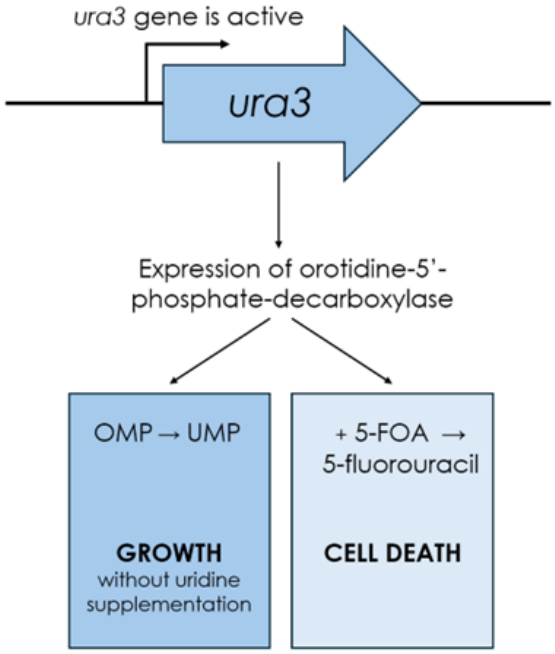

Figure 1.3.: Schematic visualization of selection technique based on uridine and 5-FOA (5-fluoroorotic acid); when orotidine 5-monophosphate (OMP) is transformed to uridylic acid (UMP) the result is a viable cell and thereby growth on media without uridine supplementation; addition of 5-FOA leads to its conversion to 5-fluorouracil, resulting in cell death

Protoplast-mediated transformation relies on activation of homologous recombination of the genes as a repair mechanism. However, the targeted deletion may not occur, because during this process non homologous end joining (NHEJ) might be favoured as a repair mechanism [26]. Both repair mechanisms are involved the repair of double strand breaks, which are induced via transformation [27][28][26].

In contrast to the non homologous end joining, homologous recombination is less prone to errors, since this repair mechanism utilizes homologous DNA as a template. By doing so a complementary strand is generated. NHEJ does not require a template, hence it can easily lead to unintended modifications [27][28][26]. By comparison of both repair mechanisms it must be noted that non homologous end joining is more efficient and faster than homologous recombination, thus often the preferred repair mechanism. Nevertheless homologous recombination is more likely to result in a correct deletion [27][28][26].

Furthermore, in order to increase the chance of inducing homologous recombination and decrease the activation of non homologous end joining the gene *dnl4* can be deleted in addition to *ura3*. *Dnl4* is encoding for a DNA ligase, essential in non homologous end joining and thereby its deletion is associated with the increased efficiency of homologous recombination [29].

1.3. CRISPR/Cas9

The genetic engineering tool CRISPR/Cas has revolutionized molecular biology and genetics in the past decade, due to its high specificity, yet easy implementation in daily lab work. The scientists Jennifer Doudna and Emmanuelle Charpentier were awarded the Chemistry Nobel Prize in 2020 for their significant and groundbreaking discovery [30].

CRISPR, abbreviated for Clustered Regularly Interspaced Short Palindromic Repeats, were described for the first time in the DNA sequence of *E. Coli* in 1987 by Ishino *et al.* [30], however their significance and origine remained unknown. Nevertheless, the occurrence of CRISPR in evolutionarily distant life domains indicated their significance. An established hypothesis, which later was successfully proven suggested, that these loci, which included intercalated foreign

DNA fragments, are involved in the immune defense of archaea and bacteria [30]. Furthermore, in 2002 Jansen *et al.* [31] established the presence of CRISPR-associated nucleases (cas genes). The genes are located in close proximity to the CRISPR locus in a plethora of prokaryotes and possess typical characteristics of nucleases [31]. The system CRISPR/Cas comprises three steps, starting with the acquisition of a protospacer, whereby foreign, originally viral, DNA is introduced within the repeating CRISPR sequence [32][30][33]. Identification and selection of a protospacer by a bacterium is based on protospacer adjacent motifs (PAMs) located downstream in the foreign DNA. The protospacer serves as a molecular memory, thus bacteria can induce a faster immune response against reoccurring viruses[32][30][33].

To form a pre-crRNA (CRISPR RNA) a sequence located in the CRISPR site is transcribed. In addition, transcription of a sequence located upstream of the CRISPR site, yields in a tracrRNA (trans-activating RNA), whereby tracrRNA and crRNA are complementary to each other and consequently a dsRNA is formed [32][30][33][34]. A cleavage induced by a RNase III leads to formation of a tarcrRNA:crRNA complex, characterized by a spacer specific to a intruding virus. This complex is often referred to as a single guide RNA [30][33][34]. Attaching of the complex to the Cas9 protein, also called loading, yields in an active ribonucleoprotein complex (depicted in Figure 1.4).

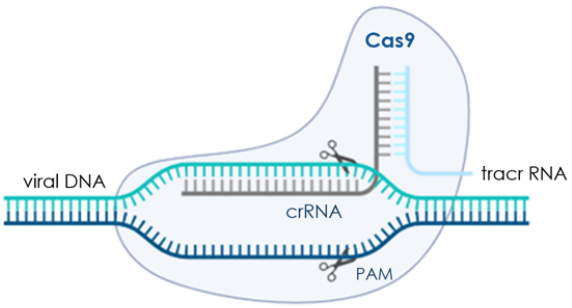

Figure 1.4.: Loaded (with tracrRNA:crRNA complex) Cas9 protein results in an active ribonucleoprotein

The active ribonucleoprotein complex can recognize and bind to protospacer adjacent motifs. In gene editing the motif 5' NGG 3' is broadly used as a recognition site for Cas9 from *Streptococcus pyogenes* [32][30]. Unwinding the DNA allows binding of crRNA the viral DNA (based on complementarity) and finally Cas9 introduces a double strand break in the viral DNA

[32][30][33][34]. Officially the system CRISPR/Cas is divided in three classes, distinguished based on phylogeny, the process of generation of Cas ribonucleoproteins and crRNA and structural differences [33]. For bioengineering purposes CRISPR/Cas class II is mainly applied and therefore studied profoundly. In contrast to other molecular tools which insert double strand breaks in the DNA, CRISPR/Cas offers a widespread utilization in different hosts. In addition this technique is inexpensive, off target effects are only moderate and it is highly efficient.

1.4. Objectives

In the scope of this work the goal is the construction of a deletion strain of *A. pullulans* EXF-150 [35], with the further perspective of obtaining a simple molecular tool for the genetic manipulation of *A. pullulans*. This should be achieved by applying two different transformation methods - protoplast mediated and chemical transformation. Furthermore, the system CRISPR/Cas9 is intended for the deletion of the gene *ura3*. Additionally the gene *dnl4* is targeted, which is supposed to increase the probability of a homologous recombination as a main DNA repair mechanism during tranformation.

2. Material & Methods

2.1. Media preparation

All media required for cultivation of of *Aureobasidium pullulans* and obtained deletion strains are listed in Table 6.2 with the recipe used for the preparation. Media was autoclaved and stored at room temperature until further required.

Table 2.1.: Media preparation for cultivation of *A. pullulan* and deletion strains; LB was used for cultivating *E.coli*

Medium	Composition
LB	1 % Peptone, 1 % Sodium Chloride, 0.5 % Yeast Extract
MAM	For 1 L total amount of MA-Medium, 20 mL 50x Trace Elements, 250 mL 2x Mineral Salts, 500 mL 0.1 M Phosphate Citrate Buffer (pH 5), 1 mL 5 M Urea, 10 g Glycerol and 1 g Peptone were added and filled up to 1 L with ddH_2O.
MEX	3 % Malt Extract, 0.1 % Peptone, 0.5 % Yeast Extract
YPD	1 % Yeast Extract, 2 % Peptone, 2 % Glucose
	If required, 1.5 % Bacteriological Agar was added.

The recipes for the preparation of 50x Trace Elements, 2x Mineral Salts and 0.1 M Phosphate Citrate Buffer for MA-Medium are provided in Table 2.2. The adjustment of pH for the 50x Trace Elements Solution to 2 is crucial. Furthermore, the pH of the phosphate citrate buffer (0.1 M) is adjusted to 5 with a 1 M citric acid solution and consequently filled up with ddH_2O to 1 L.

September 16, 2025

Table 2.2.: Recipe for 50x Trace Elements, 2x Mineral Salts and 0.1 M Phosphate Citrate Buffer for MA-Medium

Medium	Composition
50x Trace Elements	0.9 mM $FeSO_4 \cdot 7\ H_2O$, 0.31 mM $MnSO_4 \cdot H_2O$, 0.24 mM $ZnSO_4 \cdot 7\ H_2O$, 0.77 mM $CoCl_2 \cdot 6\ H_2O$, pH is consequently adjusted to 2 with HCl
2x Mineral Salts	43.8 mM $(NH_4)_2SO_4$, 58.32 mM KH_2PO_4, 4.86 mM $MgSO_4 \cdot 7\ H_2O$, 10.88 mM $CaCl_2 \cdot 2\ H_2O$
0.1 M Phosphate Citrate Buffer	For 1 L of 0.1 M Phosphate Citrate Buffer 17.8 g of $Na_2HPO_4 \cdot 2\ H_2O$ are dissolved in water, pH is adjusted to 5 with citric acid and then filled up to 1 L with ddH_2O

2.2. Strains and Cultivation Conditions

The strain *A. pullulans* EXF-150 (Gostinčar,C. et al.[35]) was used in this study. Unless stated otherwise, the strain was cultivated on MEX (Malt Extract Medium) with 1.5 % bacteriological agar at 24 °C. If required, the medium was supplied with uridine to a final concentration of 5 mM, and/or 5-fluoroorotic acid (5-FOA) was added to a final concentration of 2 mg/mL. For liquid cultures, the agitation speed was adjusted to 220 rpm.

2.3. Primer Design

To assure specific primer binding and consequently the correct construction of the designed PCR product, the following primer criteria were applied: the primer length was adjusted to 18-22 base pairs and GC-content approximately to 50 %, the melting temperatures aimed to be between 50 – 60 °C and subsequently for secondary structures, such as hairpins. In addition, ideally, at the 3' end, A and T were avoided.

All primers were constructed and designed in the scope of this work. They are listed in Table 2.3, including their corresponding sequence. Delivered lyophilized primers were prepared by adding nuclease-free water to a final concentration of 100 mM, according to the manufacturer's instructions. For PCR purposes, the primers were further diluted to 10 mM and stored at -20 °C.

Table 2.3.: Primer sequences used in the scope of this project (D781-D788)

Primer Nr.	Primer Name	Sequence
D781	Apul_ura3_5fwd	GAAGAGCGAATCCGAGCAGAG
D782	Apul_ura3_3rev	GGCCGAGACCATCTCCAGTG
D783	Apul_ura3_3fwd	AGCAGCCTCGCCTACGCCAAACCACCACGG
D784	Apul_ura3_5rev	TTGGCGTAGGCGAGGCTGCTGTCTACATG
D787	Dura3_Colony_PCR_fwd	AGTGGAGTGTTCTCAGGCAG
D788	Dura3_Colony_PCR_rev	GCCTTGGCCCTCTTATCTTG

2.4. sgRNA Synthesis for CRISPR/Cas9 Genome Editing

For the generation of the single guide RNA (sgRNA) for CRISPR/Cas9 genome editing, a suitable target site is required within the locus, which needs to be edited. The sequence (GG(N)18NGG) was identified using GeneRunner 6.0. Furthermore for optimal in vitro transcription 5'GG is essential. As a protospacer adjacent motif, also called PAM, which is a conserved, very short DNA sequence, is necessary in order for the CRISPR/Cas9 system to recognize and attach to the target DNA, which is fulfilled by the sequence 3'NGG. In order to integrate the T7 promotor sequence, as well as an additional sequence located upstream of the recognition site the online tool EnGen sgRNA Template (Oligo Designer) was used (https://sgrna.neb.com/#!/sgrna). Gene Runner was used in order to verify that no secondary structures, which potentially might lead to lower efficiency, are present.

Designed oligos (see Table 2.4) were ordered and synthetized by Mycrosynth AG and subsequently the lyophilized oligos were dissolved in RNase-free H_2O to a final concentration

of 100 µM. To obtain the final (full-lenghth) sgRNA, EnGen® sgRNA Synthesis Kit was used. Therefore the oligos were further diluted to 1 µM. In a 1.5 mL reaction tube 2 µL RNase-free H_2O, 10 µL EnGen 2x sgRNA reaction mix, 5 µL of the target specific oligo, 1 µL DTT (0.1 M) and 2 µL EnGen sgRNA Enzyme Mix were mixed and incubated at 37 °C for 30 minutes. The reaction mixture was transferred on ice and filled up to 50 µL with RNase-free H_2O. After adding 2 µL of DNase I the mixture was incubated at 37 °C for 15 minutes. The synthetized sgRNA was purified using NEB Monarch ® RNA Clean Up Kit. All steps above were performed according to the manufacturer's instructions. The sgRNA was finally eluted in 20 uL RNase-free H_2O and concentration was measured with Nanodrop.

Table 2.4.: Designed oligos and the corresponding sequences used in the scope of this project (D781-D788) for CRISPR/Cas9

Primer Nr.	Primer Name	Sequence
D785	sgRNA1_ApuI_ura3_5fwd	TTCTAATACGACTCACTATAGTCGCTGCGATCAATCGTAGGGTTTTAGAGCTAGA
D786	sgRNA2_ApuI_ura3_3rev	TTCTAATACGACTCACTATAGCTTGAGCACCGTAGACACCGGTTTTAGAGCTAGA
D719	sgRNA1_ApuI_dnl4_5fwd	TTCTAATACGACTCACTATAGTGAAGGGAAAGGTCTTGGAGTGGGTTTTAGAGCTAGA
D720	sgRNA2_ApuI_dnl4_3rev	TTCTAATACGACTCACTATAGAGTCACTCAGAGAAGGCACGAGGGTTTTAGAGCTAGA

2.5. Preparation of *E. coli* chemically competent cells

For the preparation of *E. coli* chemically competent cells 10 mL of LB were inoculated with *E. coli* Top10 (Invitrogen, Life Technologies, UK) and incubated at 37 °C at 200 rpm overnight. 100 mL of LB are inoculated with 1 mL of the overnight culture, incubated at 37 °C and 200 rpm until an OD_{600} between 0.3 – 0.4 is reached. Cells are harvested by centrifugation for 10 minutes at 4000 rpm and 4 °C. The supernatant is then discarded and 50 mL of a 1 M $CaCl_2$ solution is added and the cells are carefully resuspended. After a 15 minutes incubation on ice the centrifugation step is repeated and the cells are resuspended in 50 mL of 100 mM $CaCl_2$ solution containing glycerol (15 % v/v). Aliquots of 50 µL are prepared in Eppendorf tubes and stored at -80 °C. These steps align with standard protocols for the preparation of chemically competent *E. coli* cells [36][37].

2.6. Construction of pJET_△ura3

For cloning purposes, PCRs were performed with Q5® high-fidelity DNA polymerase with a final concentration of 0.02 U/µl, Q5® reaction buffer, and 10 mM dNTP solution mix. Primers with a final concentration of 0.5 µM were added. The reaction mixture used for the PCR reaction with Q5 Polymerase (following the manufacturer's instructions) and the setup are summarized in Tables 2.5 and 2.6. Each PCR product was loaded on a 0.8 % agarose gel and gel electrophoresis was performed (100 V/45 minutes). The desired band was cut out and the DNA was purified with NEB Monarch® DNA Extraction Kit. Finally, concentration was measured with NanoDrop One/One© UV/Vis Spectrophotometer.

Table 2.5.: Required reagents for Q5® PCR; all primers were previously diluted to a final concentration of 10 mM

Reagent	Amount [µL]
Q5® Reaction Buffer	10
dNTPs	1
Forward Primer	2.5
Reverse Primer	2.5
Q5® Polymerase	0.5
Template (5ng/µL)	1
ddH_2O	32.5
$\sum$	50

Table 2.6.: Q5® PCR Cycler Condititions (according to manufacturer), whereby the steps denaturation, annealing and extension were repeated for 30 cycles

Step	Temperature [°C]	Time [sec]
Initial Denaturation	98	120
Denaturation	98	8
Annealing	Individual for each primer	20
Extension	72	20-30 sec/kb
Final Extension	72	120
Hold	4	∞

To fuse the flanks of the gene sequence of interest, thus 5'-flank and 3'-flank, a SOE (Splicing by Overlap Extension) PCR was performed. Prior to this, both DNA fragments were amplified (using primers D781 and D785 for the 5' flank and D782 and D784 for the 3' flank) and purified separately, followed by a second round of PCR. Upstream and downstream regions were fused by the alignment of the overhangs using primers D781 and D782.

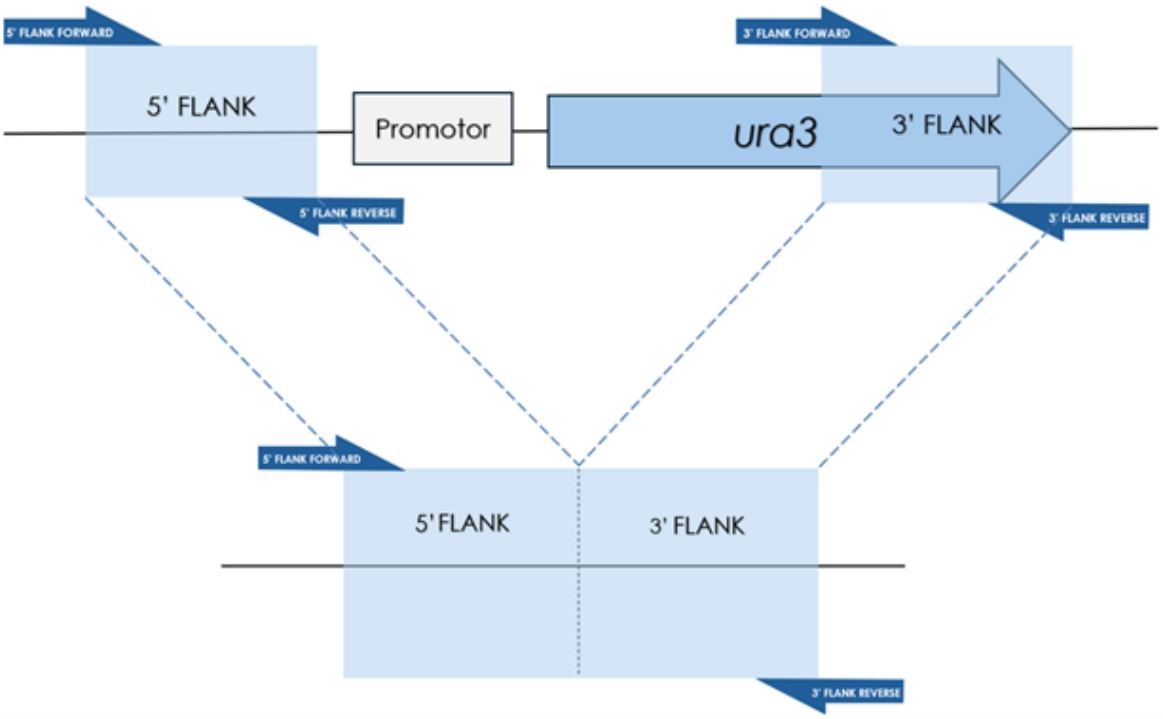

Figure 2.1.: Schematic visualization of the construction of the deletion strain Δura3

The PCR was inserted into pJET1.2 using CloneJET PCR Cloning Kit according to the manufacturer's instructions. To this end, 5 µL reaction buffer, 0.5 µL pJET cloning vector (corresponding to 25 ng in total), 0.5 µL T4 DNA Ligase and the insert (3:1 ratio of insert:vector) were pipetted in a 1.5 mL reaction tube. The mixture was incubated at RT for 10 minutes. For transformation 10 µL of the ligation mixture and 50 µL of previously prepared *Escherichia coli* Top 10 competent cells were used. The solution was incubated on ice for 30 minutes, followed by a heat shock (42 °C/2 minutes). After heat shock the reaction tube was transferred on ice and 350 µL of LB medium was added for recovery. After 30 minutes of regeneration time between 50 and 100 µL of the mixture were plated on LB agar plates with ampicillin with a final concentration of 100 mg/mL and incubated at 37 °C overnight. Potential candidates were picked and grown in 5 mL liquid cultures. After purification of the plasmid with Monarch® Plasmid Mini-Prep Kit, the resulting sequence was verified by Sanger Sequencing (Mycrosynth AG, Switzerland).

After verification by sequencing, the complete sequence of the fused fragments, pJET_Δura3, was amplified using OneTaq® Polymerase with primers B903 and B904. The reaction mixture

used for PCR reaction with OneTaq® Polymerase (following manufacturer's instructions) and the setup are summarized in Tables 2.7 and 2.8. The DNA was precipitated by adding 96 % ethanol and 3 M sodium acetate (pH 5.2), purified, and consequently used as a template for the fungal transformation.

Table 2.7.: Required reagents for OneTaq® PCR

Reagent	**Amount [µL]**
OneTaq® 5x Reaction Buffer	10
dNTPs	1
Forward Primer	2.5
Reverse Primer	2.5
OneTaq® Polymerase	0.5
Template (1ng/µL)	1
ddH_2O	32.5
$\sum$	25

Table 2.8.: OneTaq® PCR Cycler Condititions (according to manufacturer), whereby denaturation, annealing and extension step were repeated for 33 cycles

Step	**Temperature [$^\circ$C]**	**Time [sec]**
Initial Denaturation	94	30
Denaturation	94	20
Annealing	Individual for each primer	20
Extension	68	60 sec/kb
Final Extension	68	300
Hold	4	∞

2.7. Transformation

In the scope of this work two different transformation methods were applied. On the one hand protoplast-mediated transformation, which has shown high efficiency for *A. pullulans* (Kreuter *et al.* [18]), but also for other fungi like *Trichoderma reesei* and on the other hand, a chemical transformation method, which was recently published by Alison C.E. Wirhsing *et al.* for *A. pullulans* [14].

2.7.1. Transformation via Protoplasting

Protoplast-mediated transformation starts with the preparation of all required media listed in the table below (Table 2.9) [18][38]. In addition a 1.2 M Sorbitol solution was prepared. The media was autoclaved prior transformation, buffer B and 1.2. M Sorbitol were stored at 4 $^{\circ}\mathrm{C}$ and buffer A, buffer C and 60 % PEG solution at room temperature.

Table 2.9.: Required buffers for protoplast mediated transformation; after reagents are added buffers are filled up with ddH_2O until required volume is reached and autoclaved

Buffer	Reagents
Buffer A	100 mM KH_2PO_4 1,2 M Sorbit pH adjusted to 5.6 with KOH
Buffer B	1 M Sorbit 10 mM Tris.Cl (pH = 7.5) 25 mM $CaCl_2$
Buffer C	1 M Sorbit 10 mM Tris.Cl (pH = 7.5)
60 % PEG Solution (for a total volume of 100 mL)	60 g PEG 4000 1 mL 1 M Tris (pH = 7.5) 1 mL 1M $CaCl_2$ 38 mL ddH_2O Must be incubated at 50 $^{\circ}\mathrm{C}$ in order to dissolve PEG.

On day one, *A. pullulans* cells were scraped off a freshly grown plate and resuspended in 1 mL of 0.8 % NaCl / 0.05 % Tween solution. 20 mL of MEX with uridine were inoculated with the solution, OD_{600} was adjusted to 0.05, and the flask was incubated overnight at 24 °C and 220 rpm [18][38].

On the following day, the selection medium was autoclaved and stored at 55 °C until needed. Lysing solution was prepared by dissolving 650 mg of Vinotaste in 15 mL of Buffer A. After stirring for approximately 10 minutes, the enzyme solution was filtered through a 0.45 µm sterile syringe filter. The filtered solution was collected in a 50 mL falcon. Then, the OD_{600} of the overnight culture was measured, and approximately $3{\cdot}10^8$ cells were transferred to a 50 mL falcon and centrifuged at 4000 g for 5 minutes at room temperature. The pellet was resuspended in the enzyme solution, transferred into a 100 mL flask, and incubated at 24 °C and 140 rpm until protoplasts were formed. This step requires approximately 45 to 60 minutes. The protoplasts were verified by using a light microscope. During this step, RNA refolding was performed in the PCR Cycler [18][38].
When protoplasts were obtained, the solution was transferred to a 50 mL falcon and filled up to 40 mL with ice-cold 1.2 M sorbitol. After centrifugation at 3000 g/4 °C for 10 minutes, the supernatant was discarded and the pellet was resuspended in 30 mL of ice-cold sorbitol. The centrifugation step was repeated, during which the sgRNA was loaded onto Cas9. Therefore 15 µL 10x Cas9 Buffer, 4.25 µL EnGen Cas9 NLS, in total 2.7 µg sgRNA were mixed together and filled up to 150 µL with Buffer B, incubated for 10 minutes at 37 °C and stored on ice afterward [18][38].
After centrifugation was completed, the supernatant was discarded, and the protoplasts pellet was very carefully resuspended in 1 mL of buffer B. Keeping the protoplasts on ice at all times and treating them carefully is crucial for a successful transformation. For each transformation reaction, a 50 mL falcon was cooled on ice. For CRISPR/Cas9, 150 µL of Cas9 with sgRNA mixture, DNA template (Δura3), 100 µL protoplast solution, and 100 µL of 20 % PEG were mixed. If transformation was performed without CRISPR the Cas9/sgRNA mixture was substituted with 150 µL of buffer B. After incubating the transformation mixture on ice for 30 minutes, 60 % PEG was added stepwise (50, 200, and 500 µL) and incubated for another 20 minutes at room temperature. Subsequently, buffer C was added stepwise (200, 400, 1000, and 2500 µL). Prior to plating, each falcon was filled up to 50 mL with the selection medium (55 °C) and poured onto a plate. The plates were then incubated in the dark for 7 to 21 days at room temperature[18][38].

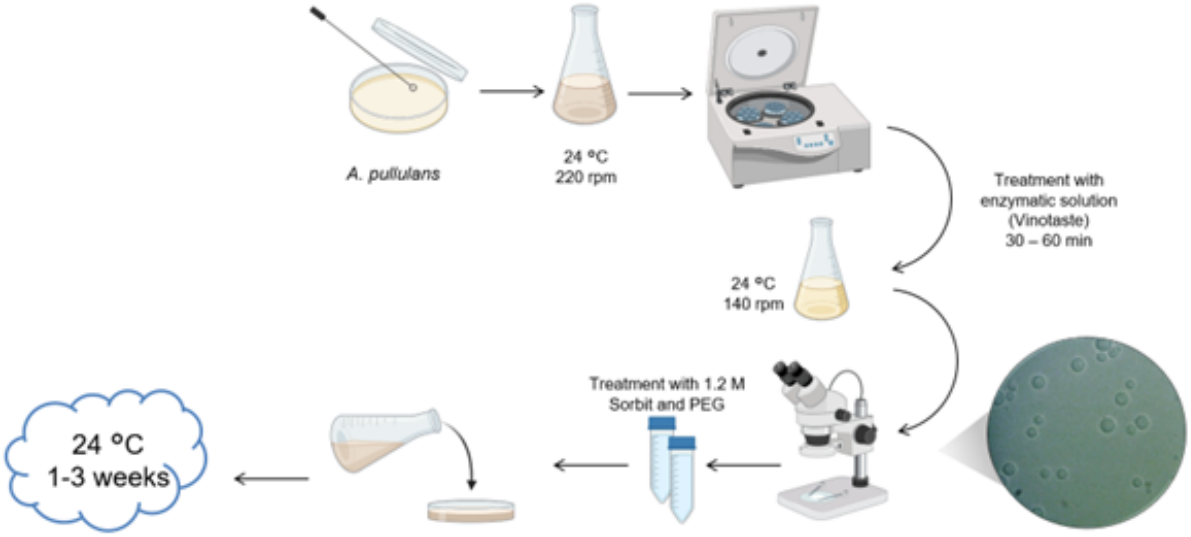

Figure 2.2.: Schematic visualization of protoplast-mediated transformation

2.7.2. Chemical Transformation

A recently published technique, by Alison C.E. Wirhsing *et al.* [14], for the chemical transformation of *A. pullulans* was applied in addition to the protoplast-mediated transformation.

Chemical transformation requires the preparation of competent cells. Therefore, 5 mL of YPD with 2 % glucose were inoculated with *A. pullulans* EXF-150 and incubated for 18 hours at 24 °C/220 rpm. After incubation, the culture was diluted with YPD with 4 % glucose to a final cell density of $5{\cdot}10^6$ cells/mL in a 250 mL flask. Cells were then grown for 2 – 3 hours at 24 °C/ 220 rpm until reaching a final cell density of 10^6 cells/mL, followed by cell harvesting by centrifugation at 2300 rpm for 8 minutes. After discarding the supernatant the pellet was resuspended in 1 mL of ddH_2O. The cells were then centrifuged at 9500 rpm for 10 seconds, the supernatant was discarded, and the pellet washed with 500 µL competence buffer. After repeating the centrifugation step, the pellet was resuspended in 250 µL competence buffer, and aliquots of 60 µL were prepared and stored at -80 °C until needed [14].

Prior transformation was performed, single-stranded fish sperm DNA (10 mg/mL) was boiled for 5 minutes in a buffer consisting of 10 mM Tris-HCl, 10 mM NaCl, and 1 mM EDTA (pH = 8) and stored at -20 °C.

Transformation starts by mixing 5-10 µg DNA (Δura3), 10 µg of fish sperm DNA, and an aliquot of competent cells. To the mixture, 2.5 µL 40 % glucose, 600 µL transformation buffer, and finally, 30 µL 40 % glucose, after each additional component, the tube was flicked in order to mix the reagents. The mixture was then incubated for 1 hour at 24 °C/300 rpm, followed by heat shock (15 minutes at 37 °C). The cells were harvested by centrifugation at 9300 rpm for 30 seconds. The supernatant was then discarded and the pellet was resuspended in 1 mL of 1 M Sorbitol. After mixing by flicking 1 mL YPD with 2 % glucose was added. Cells were left to recover for 4 hours at 24 °C/100 rpm, and 50 µL were plated on selection medium plates. Plates were incubated at room temperature for 2 to 5 days [14].

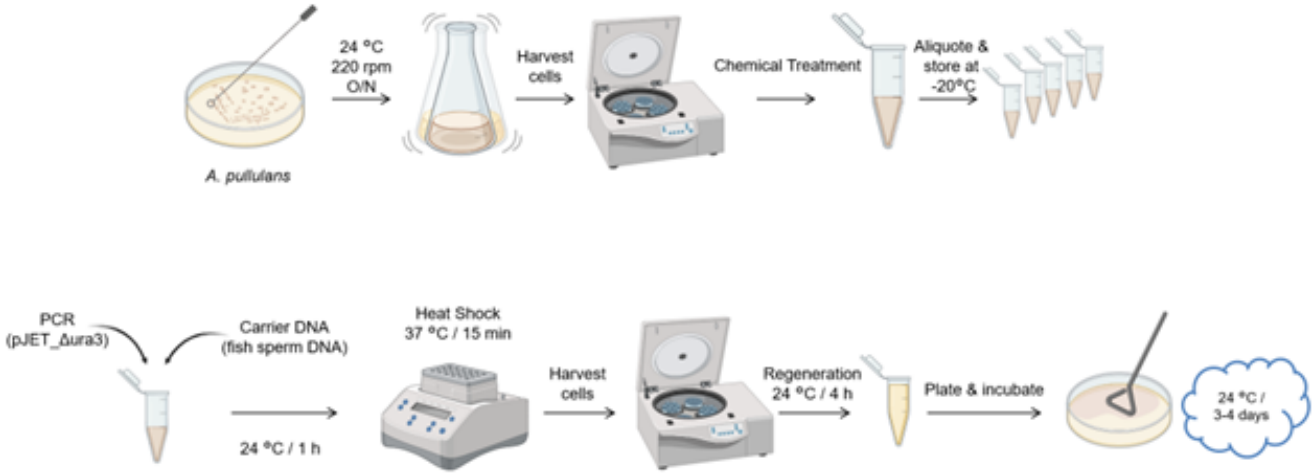

Figure 2.3.: Schematic visualization of chemical transformation

2.8. Extraction of chromosomal DNA

For the extraction of chromosomal DNA first screw cap reaction tubes filled with glass beads (0.37 g of 0.5 mm glass beads, 0.25 g of 1 mm glass beads and one large (5 mm) glass bead) were prepared and filled with 1 mL of CTAB buffer (Recipe in Table 2.10, prior autoclaving buffer was heated up at 63 °C in a waterbath for all components to dissolve). Approximately 50 mg of mycelium were transferred into the tube and the spores were disrupted by using the FastPrep-24™ Classic bead beating grinder and lysis system (30 seconds at level 6). The reaction tube is incubated at 65 °C for 20 minutes and the supernatant is transferred to a new 2 mL reaction tube. After adding 400 µL of phenol and mixing the solution, another 400 µL

of chloroform is added. The reaction tube is then incubated for 10 minutes and centrifuged at 1200 g/4 °C for 10 minutes. After centrifugation is completed, approximately 650 µL of the aqueous phase is transferred to a new 1.5 mL tube, and subsequently, 650 µL of chloroform is added. After mixing the reaction solution, the centrifugation step is repeated. 500 µL of the aqueous phase is transferred to a new 1.5 mL tube, and 1.5 µL of RNase A (10 mg/mL) is added. The reaction is incubated at 37 °C for 30 minutes. In order to precipitate the DNA, 350 µL of isopropanol is added, followed by incubation at 4 °C for 30 minutes. The solution is then centrifuged at 25 000 rpm and 4 °C for 1 hour. The supernatant was discarded, and the pellet was washed with 1 mL of 70 % ethanol. The centrifugation step was repeated for 10 minutes, and the supernatant was removed. In order to evaporate the ethanol and water residues the pellet was dried at 50 °C. Finally, it was dissolved in 20 – 30 µL ddH_2O, and concentration was measured using a NanoDrop One/One© UV/Vis Spectrophotometer.

Table 2.10.: CTAB buffer recipe for 100 mL was prpepared as followed: 8.15 g NaCl, 1 g Polyvinylpyrrolidone, 2 mL 0.5 M EDTA, 10 mL 1 M Tris.Cl and 2 g CTAB; all components were dissolved at 63 °C in a waterbath prior autoclaving)

Reagent	Concentration
NaCl	1.4 M
Tris.Cl (pH=8)	100 mM
EDTA	100 mM
CTAB	2%
Polyvinylpyrrolidone	1%

2.9. Genotyping

In order to confirm positive transformants, a PCR using OneTaq® Polymerase was performed (see Table 2.7 and 2.8). The previously extracted chromosomal DNA was used as a template. Thus, concentration was adjusted to 1 ng/µL. As a negative control instead of DNA, ddH_2O was used. For the PCR primers D787 and D788 were used.

After the PCR, 6x Loading Dye (Thermo Scientific™, Germany) was introduced to the solution and the mixture was loaded onto a 0.8 % gel. Subsequently a gel electrophoresis was performed, adjusting the settings to 100 V and 45 minutes running time. For visualization of the gel the ChemiDoc™ Touch Imaging System was used.

To ensure that the chosen transformants are not false positive and to confirm that deletion occurred at the desired locus for some of the samples the PCR was repeated with Q5® high-fidelity DNA polymerase and sent for sequencing (Sanger Sequencing, Mycrosynth AG, Switzerland). The primers D787 and D788 were diluted according to the sampling requirements of Mycrosynth AG. The primers each bind approximately 100 bp prior to and after the desired sequence, assuring an integration at the right locus. The obtained results were then compared to the reference sequence of the wild type.

3. Results

3.1. Construction of pJET_△ura3

In Figure 3.1 and Figure 3.2 the PCR products loaded on a 0.8 % agarose gel visualized via the ChemiDoc™ Touch Imaging System are shown. The 5' flank and 3' flank are both at approximately 300 base pairs (Figure 3.1). After fusing the flanks together, the product is at approximately 600 base pairs (Figure 3.2).

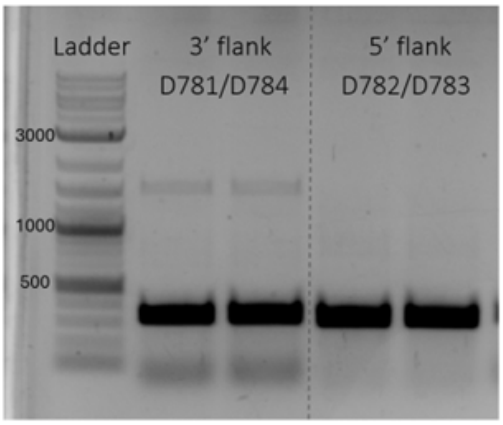

Figure 3.1.: Construction of 5' and 3' flank (*ura3*) via PCR

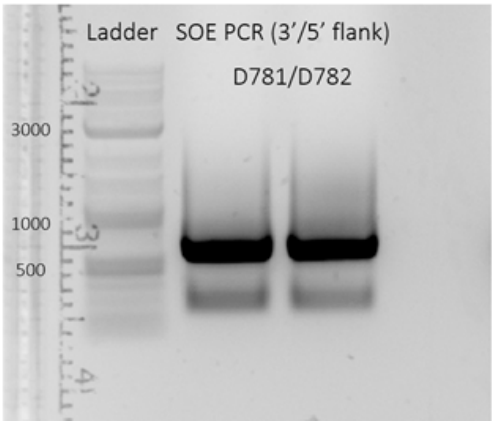

Figure 3.2.: Constructed △ ura3 after SOE PCR (fusion of previously obtained 5' and 3' flank)

3.2. Transformation via protoplasting

The first colonies appeared approximately 7 to 21 days after transformation. Their color was in the range between off-white and pale brown, and in addition, they were sticky, presenting the typical phenotype of *A. pullulans* on MEX (see Figure 3.3,a). A longer incubation period resulted in more colonies. However, they seemed to grow slower compared to the first colonies that appeared. On the negative control, no colonies were visible (Figure 3.3,b), indicating a successful transformation. Suspected positive transformants were cut out and transferred to a fresh selection medium plate to grow prior to extracting the DNA.

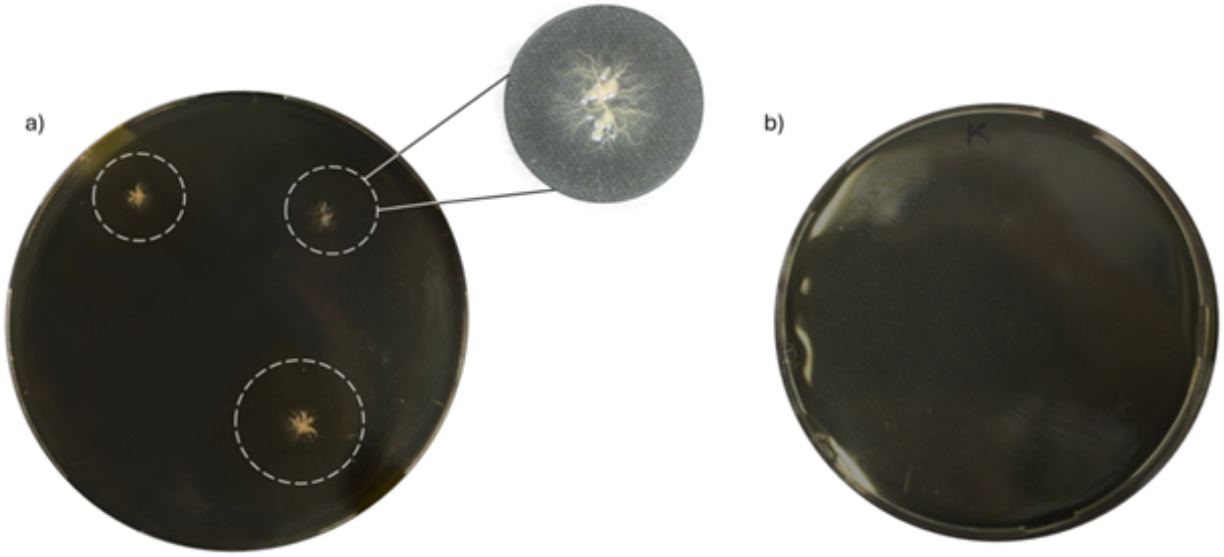

Figure 3.3.: *Aureobasidium pullulans* transformants plated on MEX supplied with Uridine; a) obtained transformants; b) negative controll with water added instead of DNA)

3.3. Chemical Transformation

After incubating the plates for two to five days, the first, creamy white and round colonies appeared, as shown in Figure 3.4,a. By incubating the plates for longer periods of time, the background turned black, indicating melanin production, associated with *Aureobasidium* (Figure 3.4,b).

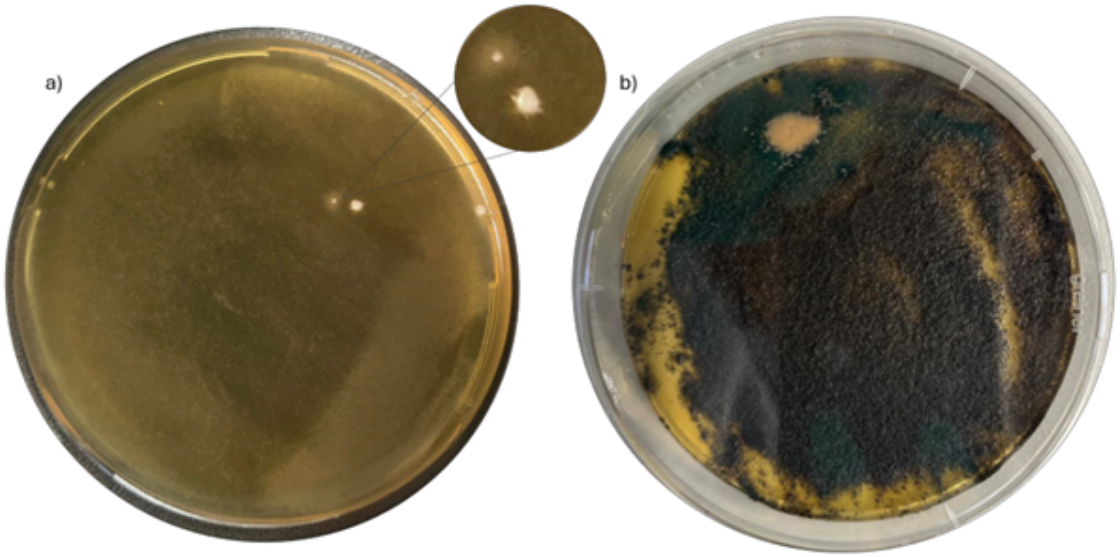

Figure 3.4.: *Obtained transformant after chemical transformation; a) after incubation time of 2-3 days b) after incubating the transformation plates at least for 5 days (they turn black)*

The transformants were observed under the light microscope (at a magnification of 40x), whereby a round, swollen structure was observed (Figure 3.5.). This structure reminds of a ascus-like structure, since, as shown on the right of Figure 3.5, it seems to burst and release, what appear to be bubbles. This bubbles could be interpreted as asco-spores, however further analysis is required. Such a structure might indicate a sexual form (teleomorph) of the yeast-like fungus, which has not been described yet. Despite of different attempts to isolate this structure, when observed under light microscope its wall was already destroyed. It is important to mention that this structure, slightly reminding of an ascus, was only observed after a chemical transformation was performed and after two to three days of incubation, before the plate turned completely black, indicating the production of melanin.

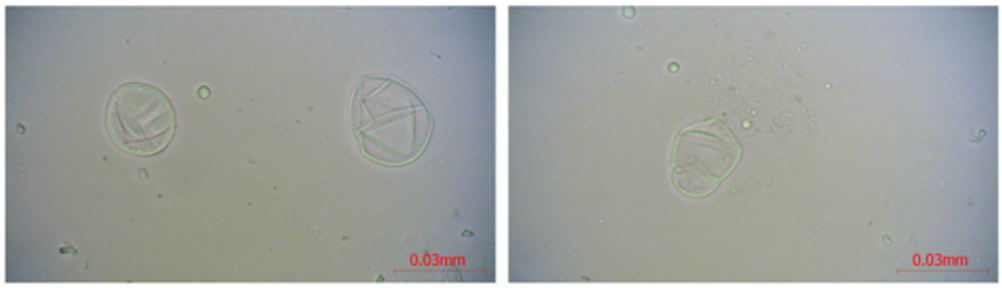

Figure 3.5.: Swollen roundish structure, which was observable after chemical transformation

3.4. Calculation of colony forming units per microgram (CFU/µg)

For the comparison of the applied transformation techniques the colony forming units per microgram were calculated by the equation given below:

$$CFU/\mu g = \frac{Colony\ forming\ units \cdot Volume\ of\ media\ after\ recovery\ [\mu L]}{Plated\ volume\ [\mu L] \cdot DNA\ amount\ [\mu g]} \tag{3.1}$$

For each transformation technique, in total five plates after transformation were taken into consideration for the calculation of CFU/µg, whereby the final value is obtained from averaging the results. For the protoplast mediated transformation the colony forming units were counted at day ten ad for the chemical transformation at day four. Furthermore, it must be pointed out, that the equation for calculating the colony forming units per microgram for the protoplast mediated transformation was simplified, since the volume of the media after recovery and the plated volume are the same. Thus to obtain the CFU/µg the colony forming units are divided by the DNA amount (in µg) added.

Protoplast-mediated transformation yielded in approximately 7 CFU/µg when 2 µg of DNA were added and approximately 5 CFU/µg if 5 µg or 7 µg of DNA were added, indicating a decrease of CFU/µg when introduced DNA amount was increased.

In contrast to the protoplast-mediated transformation, chemical transformation yielded in approximately 57 CFU/µg, when 10 µg of DNA were added.

3.5. Verification of positive transformants

In total approximately 100 colonies, resulted from the protoplasts-mediated and chemical transformation, were tested via PCR (using primers D787 and D788). In Figure 3.6 and 3.7 nine of the tested colonies, are presented.

Firstly, depicted in Figure 3.6, OneTaq® Polymerase was used, which resulted in additional unspecific bands. As a negative control, for an unsuccessful transformation, the wild type (WT) was used. The corresponding band was at approximately 2000 base pairs. The candidates one to five were colonies picked after protoplast-mediated transformation was performed. Number six to nine were transformants obtained from the chemical transformation. The band from a successful deletion was expected to be at approximately 907 base pairs.

In order to avoid unspecific binding of the primers (visible in Figure 3.6), a second PCR was performed using Q5® high-fidelity DNA polymerase (Figure 3.7), which successfully resulted in a single, specific band. For all tested colonies, the PCR indicated that the transformation was not successful.

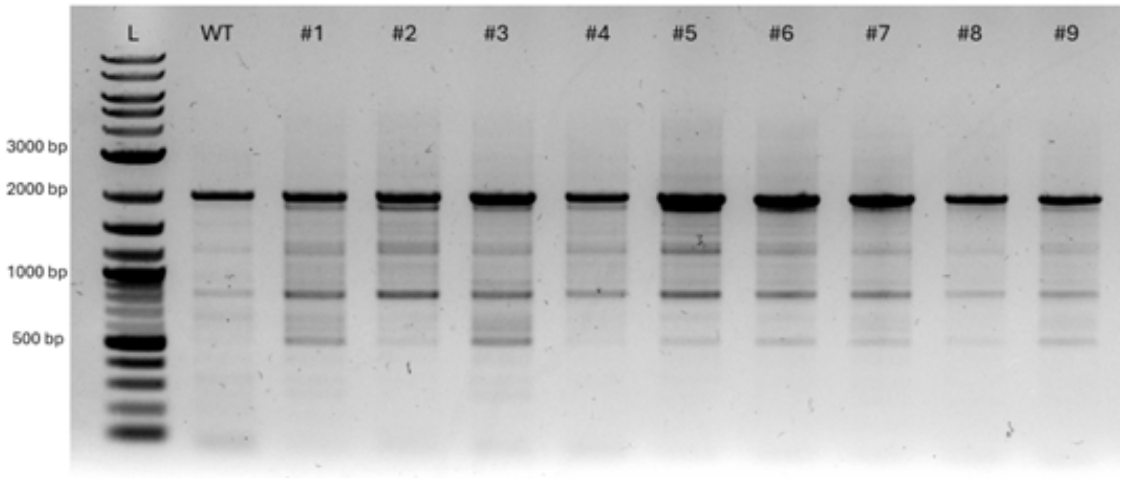

Figure 3.6.: *Aureobasidium pullulans* colonies were picked from the transformation plates after protoplast-mediated transformation was performed; after isolation of DNA were tested by PCR with OneTaq resulting in unspecific binding of the primers (with primers D787 and D788); Wild Type (*A. pullulans* EXP 150) used as a control, since a product with this size would indicate an unsuccessful transformation

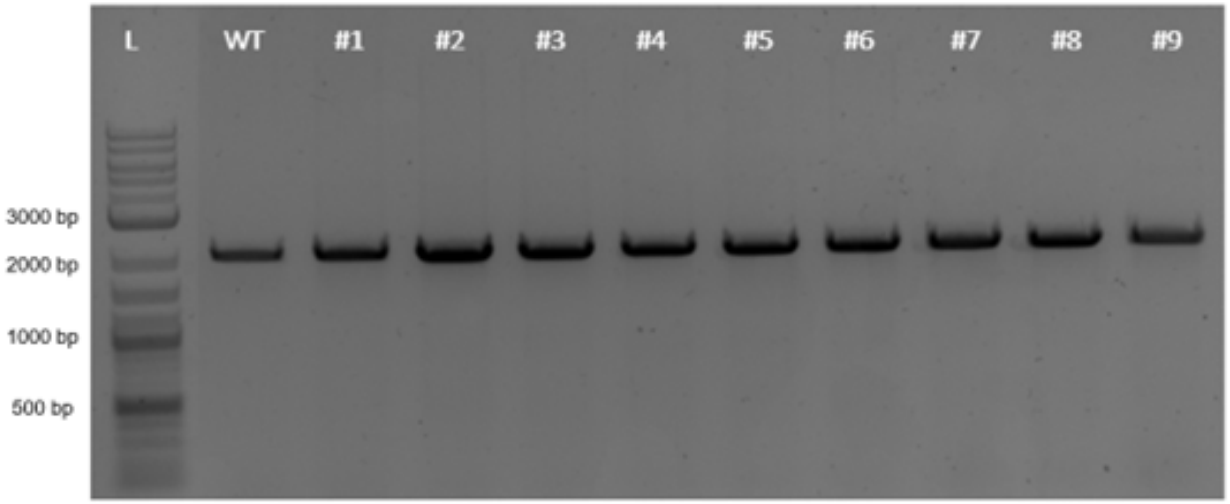

Figure 3.7.: Previously performed PCR for confirmation of positive transformants was repeated with Q5 resulting in specific binding of the primers (with primers D787 and D788); the Wild Type was used as a control, since a product with this size would indicate an unsuccessful transformation

To verify that the transformation was indeed not successful the samples were send for sequencing and the results for a single colony (obtained from a protoplast-mediated transformation) are shown in Figure 3.8. It can be noted that the alignment shows a single mutation, where cytosine is exchanged to adenine (at position 74). In total 12 candidates were sent for sequencing (one half obtained from the chemical transformation and the other one from protoplast-mediated transformation) and 8 out of 12 delivered the same outcome.

The sequencing results deliver very high accuracy for approximately 1000 base pairs in forward and reverse directions. A significant error increase, however, can be observed towards each end of the reads, which is a typical sequencing phenomenon. Such an accumulation of errors commonly arise from the decrease in signal quality, which can be justified by increased background noise, but also the depletion of the used reagents and formation of secondary structures [39][40].

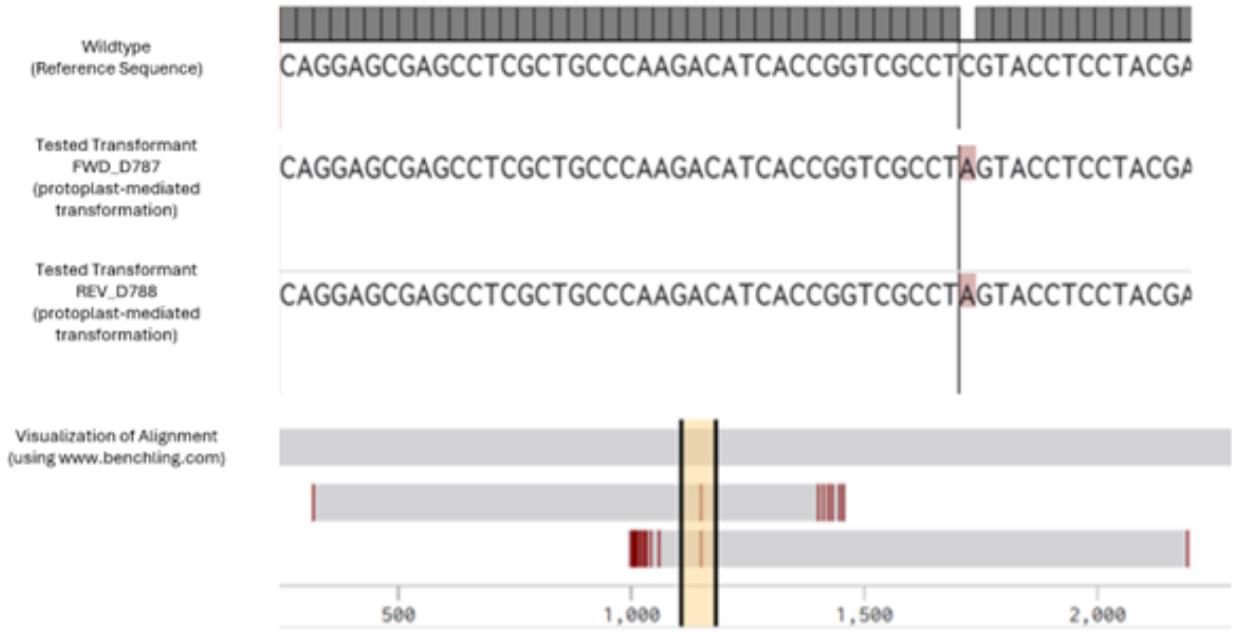

Figure 3.8.: Sequencing results of one of the picked colonies after protoplast mediated transformation; it is visible that cytosine has been replaced for adenine during transformation

The substitution of the base cytosine to adenine leads to amino acid substitution, more precisely cysteine is substituted for alanine (see amino acid sequence in Figure 3.9). This, by transformation induced mutation, is classified as a missense mutation [41], which often results in a non-functional protein.

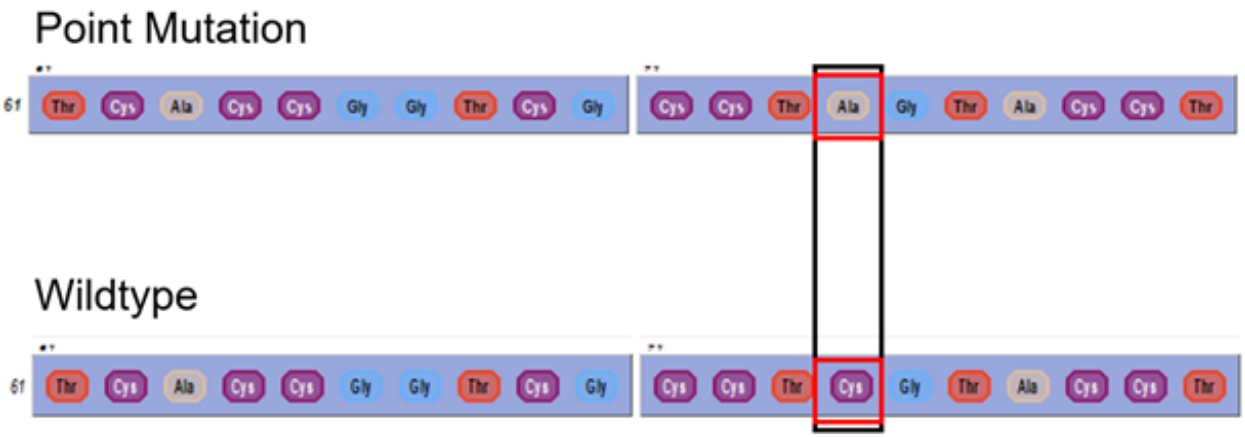

Figure 3.9.: Visualization of the point mutation – amino acid sequence: cysteine is being substituted by alanine

By comparing the amino acids, several differences can be observed – cysteine is larger than alanine and it possesses a thiol group, in contrast to alanine which has a methyl group. The difference in the chemical structure can lead to an alteration of the protein function. Thiol groups often engage in redox reactions and are equipped to form disulfide bounds [42]. Furthermore sulfur can act as a nucleophile, whereas alanine is a non-polar amino acid and due to the absence of a thiol group, it is less reactive than cysteine [43][44][42].

Figure 3.10.: Chemical structure of cysteine (left) and alanine (right)

In addition the wild type was sent for sequencing to verify that the missense mutation did not occur in the parental strain, before transformation occurred. Furthermore some of the candidates were transferred to selection medium without uridine, where they still were able to grow, indicating that the strain was still uridine prototroph.

4. Discussion

In the scope of this work the goal was the deletion of *ura3* in the yeast-like fungus *Aureobasidium pullulans* by performing two different transformation methods. In the course of which, the transformation methods and resulting transformants were to be compared and evaluated. Both transformation techniques resulted in growth on the chosen selection medium (MEX supplemented with 5-FOA and uridine) and the negative controls remained colony free. Sequencing results revealed that the applied transformation methods lead to a missense mutation (in most cases) instead of the desired deletion, if CRISPR/Cas9 was applied. These unexpected results emphasizes concerns regarding transformation techniques and their efficiency.

In order to increase the probability of a successful deletion of *ura3* and decrease of efficiency of non homologous end joining, in addition the gene *dnl4* was targeted for a deletion by using CRISPR/Cas9. The nonetheless occuring missense mutation highlights an issue often arising during transformation - the process is often accompanied by repair mechanisms prone to mistakes. These results further indicate that during transformation predominantly non homologous end joining occurred as a repair mechanism.

Despite expecting otherwise, protoplast-mediated and chemical transformation resulted in growth on selection medium, which after sequencing, could be explained by the introduced missense mutation. The mutation, which resulted in amino acid substitution (Cystein $\rightarrow$ Alanine) might lead to alteration of protein function or loss of function.

The missense mutation was introduced in close proximity to the expected cut site of Cas9 and thereby at the locus were the double strand break was intended, indicating that the mutation was Cas9-induced. This suspicion is further supported by similar data published by F. Allen *et al.* in 2020 [45], revealing mutations directly connected to Cas9 activity. This type of induced mutation could be a consequence from inaccurately executed DNA repair, commonly the case when NHEJ is applied as a repair mechanism [45]. Commonly the mutation is induced approximately three to four nucleotides upstream from the PAM locus [45].

September 16, 2025

Furthermore no additional base deletions or insertions were observed and it was established that the mutation occurred in a consistent manner, thus not random. Likewise, this connection was observed by F. Allen *et al.* [45], which strongly supports the proposed hypothesis, however the principals behind favouring a specific mutation have not been fully understood yet. Regarded from an evolutionary perspective, a mutation could be preferred, when conferring a certain advantage in growth under given selective conditions (which are provided during transformation).

A study published in Natrure, 2024 by J. Klimm *et al.* [46], using *S. cerevisiae* as a model organism, suggests that missense mutations, leading to loss of function, are induced as a response for short-term evolution, facilitating adaptation of the organism to environmental changes. In analogy to this study, it can be stated that selection media act as a stressor and is presented as a change in environment, whereby the organism is required to adapt rapidly.

Another possible explanation for the reoccurrence of the mutation, whereby cytosine is substituted for adenine, is delivered when the physiology of the cells is taken into consideration [47]. A variety of cellular and metabolic processes are controlled by reactive oxygen species (also called ROS), whereas guanine is most susceptible among all nucleic acid bases towards reactive oxygen species [47]. Thus it can produce 8 - oxoguanine, which again is most likely to pair with the purine base, adenine.

The difference in size and chemical properties of cysteine and alanine might be a further explanation for the different behaviour of the transformants in contrast to the wild type and why they are able to grow on selective conditions. If cysteine has a key role in the active sites (binding and catalytic site), the change of chemical properties is a possible explanation for this change in behaviour. Furthermore this change can have an impact on the structural features of the protein. However, in order to confirm this, further experiments, in the field of structural and functional proteomics, must be carried out.

In addition to that further transformation techniques for *Aureobasidium pullulans* could be tested and compared. Eventually protocols should be optimized and standardized in order to achieve high efficiency. Optimization starts with the design of the primers used, targeted genes and locus and used reagents. In this case, parameters such as flank length and amount of DNA utilized, can be varied in the search for an optimum.

For both transformation methods the colony forming units per microgram were calculated and in comparison to the chemical transformation, the protoplast mediated transformation yielded in a considerably lower colony forming units. Chemical transformation resulted in approximately 57 CFU/µg, which is comparable to published data by Alison *et al.* [14]. However, it must be emphasized that the direct comparison of colony forming units across different transformation methods is not very accurate, due to the fact that the techniques are highly distinct. Two major examples are incubation time - colonies were counted at day four for the chemical transformation and day ten for the protoplast mediated transformation and the reagents - chemical transformation was mainly performed with YPD and fish sperm DNA was applied, whereas protoplast mediated transformation operated mainly in MEX.

Furthermore, a study with *A. pullulans* published by A. Masi *et al.* in 2024 [48], encountered similar difficulties – a protoplast mediated transformation with CRISPR/Cas9 resulted in colonies with the expected phenotype, however these were resistant to the selected antibiotic (hygromycin), as well as to 5-FOA [48]. They further established, that an increase of template DNA did not have any significant effect on the transformation outcome.

At this point, it must be further noted that the transformants, which were subjected to transformation with CRISPR/Cas9 with the intention to delete *dnl4* were not verified by PCR or sequencing. Nevertheless, it remains to be investigated if the deletion was successful.

Eventually it can be concluded that, by their very nature, transformation methods act as a stressor for all living organisms. They can activate various repair mechanisms, aiming for survival in a changing habitat. Stress induced mutagenesis is one of the tools they posses in their survival kit, allowing adaptation [49]. From evolutional point of view these events make perfect sense and justify the growth of *A. pullulans* under selection conditions.

PROJECT B

Role of Dia3 in the biosynthetic pathway of diaporthinic acid

Abstract

The filamentous, mesophilic, saprophytic fungus *Trichoderma reesei* is one of the most potent modern hosts for the industrial production of a plethora of enzymes and proteis. Nevertehless, for the past decades research focused on the properties of secondary metabolites due to their importance. Secondary metabolites are often encoded by biosynthetic gene clusters (BGCs) and mainly produced when the microorganism has limited resources, enabling survival in harsh conditions. The *dia* BGC has aroused the interest of researchers, because of the potential antifungal and antimicrobial activities of the involved metabolites. In *T. reesei* the *dia* BGC has yet not been extensively studied and to gain some insight in the *dia* BGC, activation of the cluster is required. Therefore, *diaR1*, encoding the zinc cluster protein, was previously overexpressed by positioning the coding region under the regulation of the TEF1 promotor, resulting in the overexpression strain designated OEdiaR1. Furthermore, OEdiaR1 deletion mutants were constructed and their transcript levels were analysed.

A wild type (QM6a $\triangle$mus53) deletion mutant was constructed, whereby the gene *dia3* was deleted. For this purpose a hygromycin split marker strategy was applied. Further comparison of the strains involved growth analysis by microscopy. In addition, the dry cell weight, and tehreby the biomass production, was compared for all deletion strains to the wild type.

In the scope of this work it was revealed that, the lowest transcript abundance values were observed, when *dia3* is deleted. This outcome was supported by visual comparison of all strains, whereby it was observed that the deletion strain $\triangle$dia3 has an impaired growth. This indicates the significance of *dia3* in the *dia* BGC. Furthermore, visual and microscopic analysis revealed a slight growth impairment due to the over expression of the *dia* BGC (OEdiaR1), indicating a mild growth inhibition due to the activation of the *dia* BGC. This again seems to be counteracted by the deletion of *dia1*.

These findings empahsize the significance of the gene *dia3* in the *dia* BGC and show the complexicity of the metabolic pathway for the production of diaporthinic acid, contributing to a better understanding of the *dia* BGC.

Kurzfassung

Der filamentöse, mesophile, saprophytische Pilz *Trichoderma reesei* ist einer der potententesten modernen Wirte für die industrielle Produktion von Enzymen und Proteinen. In den letzten Jahren fokusiert sich die Forschung deutlich mehr auf die Charakterisierung und auf das bessere Verständnis von Sekundärmetaboliten, aufgrund ihrer diversen biologischen Eigenschaften. Häufig werden diese von biosynthetischen Genclustern (BGCs) kodiert und hauptsächlich dann produziert, wenn der Mikroorganismus nur über begrenzte Ressourcen verfügt, um unter rauen Bedingungen überleben zu können.

Der *dia* BGC hat das Interesse der Forscher geweckt, da die beteiligten Metaboliten potenziell antimykotische und antimikrobielle Wirkungen haben. In *T. reesei* wurde der *dia* BGC noch nicht umfassend untersucht, und um Einblicke in den *dia* BGC zu gewinnen, ist eine Aktivierung des Clusters erforderlich. Daher wurde *diaR1*, das für das Zinkclusterprotein kodiert, zuvor durch Positionierung der kodierenden Region unter der Regulation des TEF1-Promotors überexprimiert, was zu dem als OEdiaR1 bezeichneten Überexpressionsstamm führte. Darüber hinaus wurden OEdiaR1-Deletionsmutanten konstruiert und ihre Transkriptionsniveaus analysiert.

Ein Wildtyp-Deletionsmutant (QM6a $\triangle$mus53) wurde konstruiert, wobei das Gen dia3 deletiert wurde. Zu diesem Zweck wurde eine Hygromycin-Split-Marker-Strategie angewendet. Der weitere Vergleich der Stämme umfasste eine Wachstumsanalyse aller Stämme mittels Mikroskopie. Darüber hinaus wurde das Trockenzellgewicht der Biomasseproduktion aller Deletionsstämme mit dem Wildtyp verglichen.

Im Zuge dieser Arbeit wurde gezeigt, dass der *dia3* Deletionsstamm die niedrigsten Transkript-Expresisonswerte aufweist. Dies wurde weiters durch eienn visuellen Vergleich aller Stämme bestätigt, da sich der Stamm $\triangle$dia3 durch ein beeinträchtigtes Wachstum auszeichnet. Dies weist auf die Bedeutung von *dia3* im *dia* BGC hin. Darüber hinaus ergab die visuelle und mikroskopische Analyse eine leichte Wachstumsbeeinträchtigung aufgrund der Überexpression des *dia* BGC (OEdiaR1), was auf eine leichte Wachstumsinhibierung aufgrund der Aktivierung des *dia* BGC hindeutet. Dies scheint wiederum durch die Deletion von *dia1* revidiert zu werden.

Diese Ergebnisse betonen die Bedeutung des Gens *dia3* im *dia* BGC und zeigen die Komplexität des Stoffwechselwegs zur Produktion von Diaporthinsäure, was zu einem besseren Verständnis des *dia* BGC beiträgt.

September 16, 2025

5. Introduction

The filamentous fungus *Trichoderma reesei* (obsolete designation: *Hypocrea jecorina*, referring to the teleomorph) is one of the most potent modern “machineries” for the industrial production of a plethora of enzymes and proteins [50]. Over the last decades it has gained significance, especially due to its ability to degrade cellulose (cellulases), drawing the attention of biorefining and biofuel industry and its potential in the production of biofuels [51][50].

The ascomycota *T. reesei* is a mesophilic fungi, which obtains nutrients mainly from decaying organic matter, thus a saprophyte. During World War II on the Solomon Islands it was isolated for the first time from decomposing tents belonging to the US Army. Officially it was identified as *Trichoderma viride*, and the strain was named QM6a [51][52]. In 1977 during the Second International Mycological Congress the scientist E.G. Simmons revealed that the strain QM6a was distinct from the reference strain available for *T. viride* and was therefore renamed to *T. reesei*, after the mycologist that firstly isolated the strain – Elwyn T. Reese [51][50].

In order to gain better understanding of the cellolytic properties of *T. reesei*, the genome of QM6a was successfully sequenced in the year 2006 and officially published in 2008, revealing a total length of 34 Mbp and seven chromosomes [50]. It was the first strain of *Trichoderma reesei*, which was completely sequenced [50].

Since the nineties *T. reesei* played a significant role as a production host in the industry, not only because of the plethora of proteins that can be produced, but also because of its outstanding production rates. Naturally various *T. reesei* strains can reach production rates of around 30 g/L (e.g. RUT-C30), however when the strain is genetically modified and improved production rates can reach up to 100 g/L [50][53]. Furthermore the reference strain QM6a, which is the base for all industrially utilized strains, fulfills all necessary requirements regarding safety, capacity and robustness [53]. *Trichoderma reesei* is not pathogenic for humans and thus considered safe. Moreover *T. reesei* is very popular, because of its exceptionally high capacity, which can be even further improved by genetic modifications. Furthermore, commonly applied promotors such as *cbh1* can facilitate the secretion of a targeted product. Finally, *T. reesei* does not

require complex sugars (or other carbon sources), it can be cultivated easily and cheap, which makes it a perfect production host of an economic and industrial point of view [53].

Cellulases, Proteases and Glucoamylases are some of the many examples among the industrially produced enzyme classes by *T. reesei*. Cellulases are mainly known for their ability to break the glycosidic bond in cellulase and are therefore predominantly used in the textile industry [53][51]. Proteases are a crucial ingredient of every detergent and glucoamylases are frequently encountered in the biofuel industry, due to their ability to break down starch to glucose, followed by fermentation to ethanol.

Until 2021, approximately 200 enzyme products were commercially produced by means of fermentation, a fifth of which were solely produced by *Trichoderma* as a industrial host [50][53], thus again underlines the significance of the fungi in biotechnology.

5.1. The *dia* biosynthetic gene cluster in *Trichoderma reesei*

While the filamentous fungi has been extensively studied for its role in protein and enzyme production, including its primary metabolism, little is known about its ability to produce secondary metabolites. For the past decades many studies focused on the properties of secondary metabolites due to their importance. A well-known example for secondary metabolites are antibiotics, such as penicillin, which is produced by the fungus *Penicillium chrysogenum* [54]. Nowadays, with antibiotics resistance becoming a serious challenge for medicine, it is even more crucial to explore which alternatives exist.

Secondary metabolites are often produced when the microorganism has limited resources, for instance limited nutrients, enabling its survival in harsh conditions. They are often encoded by biosynthetic gene clusters (BGC), which, in simple terms, is a group of genes located in a row in a genome, typically encoding for all elements involved in a pathway to produce a secondary metabolite. Polyketides and polyketide derived isocoumarins, are a group of natural products, commonly produced by fungi [55]. Typically they are encoded by biosynthetic gene clusters, which, under normal conditions are mostly silent, therefor the metabolites are not produced. In order to activate a silent BGC in the search for new secondary metabolites, which might be of scientific interest, epigenetic regulation can be in- or decreased [56]. Eventually this can lead to

changes in the transcription of the targeted BGC at chromatin level and provoke an alteration of histones. A different technique is the overexpression of a transcription factor, that is connected to the silenced BGC and regulates the expression of the genes within this BGC [56][55]. The second approach is commonly applied as a tool to study BGCs and involvement of the genes in pathways resulting in the production of secondary metabolites.

In 2012, Nakazawa *et al.* activated the silent *aoi* BGC, with a total length of 50 kb and consisting of 14 genes – *aoiA* to *aoiO*, associated with the production of polyketides in *Aspergillus oryzae* [56]. With *aoiG* encoding for a polyketide synthase, they speculated that the enzyme was involved in the synthesis of a nephtalene backbone. In order to shed light on the *aoi* BGC they overexpressed the transcription factor AoiH (*aoiH*). Overexpression of the transcription factor revealed the production of a derivate of diaporthin and orthosporin. Another study conducted by Chankhamjon *et al.* [57] investigating the introduction of not activated carbon atoms [57] stumbled upon the unique ability of *A. oryzae* to produce chlorinated polyketides, with dichloro-diaporthin as the primary product. They revealed that *aoiQ* (part of the *aoi* BGC) encoded for a bifunctional enzyme, the flavin dependent halogenase – methyltransferase (FDH-MT), which enables the chlorination of polyketide derivates, such as orthosporin.

Due to its unique bifunctionality, a fusion of a halogenase and a methyltransferase, in 2021 M. Liu *et al.* further investigated *aoiQ* (encoding for FHD-MT) [58]. Examination of the genes close to *aoi*Q revealed that it is located in a different BGC – the *dia* BGC, encoding for a non-reducing polyketide synthase, a lactamase-like protein, a flavin dependent monooxygenase and a short chain dehydrogenase/reductase. Comparison with a genome database showed that the BGC is highly conserved.

In *Saccharomyces cerevisiae* expression of the *dia* genes revealed that the cluster yields in the production of dichlorodiaporthin and 8-methyldichlorodiaporthin, aligning with previous findings (Chankhamjon *et al.*, [57]). Furthermore, it was shown that the methyltransferase domain of the bifunctional enzyme is capable of catalysing methylations at O-6 and O-8 position resulting in 8-methyldichlorodiaporthin as the primary product [58].

The *dia* BGC has awaken the interest of the research community because of the potential antifungal and antimicrobial activities of the involved metabolites. Moreover the uniquely

asssembled enzyme FDH-MT stands out as a bifunctional enzyme. In *T. reesei* the *dia* BGC has yet not been extensively studied, nevertheless it has been established that it encodes a polyketide synthase (PKS, *dia1*), lactamase-like protein (*dia2*), dehydrogenase (*dia3*), FAD dependent oxidoreductase (*dia4*), flavin dependent halogenase – methyl transferase (FDH-MT, *dia5*) and zinc-cluster protein (*diaR1*) (see Figure 5.1).

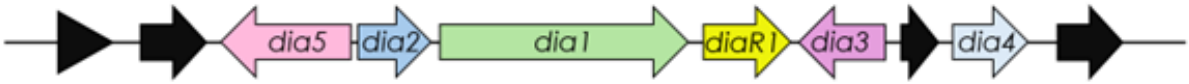

Figure 5.1.: Visual representation of the *dia* BGC and the involved genes

5.2. RT-qPCR

Reverse transcription quantitative polymerase reaction, abbreviated as RT-qPCR, is a commonly used technique for the detection and quantification of RNA [59][60]. The first step consists of the transcription of (messenger) RNA to cDNA, which then serves as a template for the quantitative polymerase chain reaction (qPCR).

The detection of the amplified product is based on fluorescence or emission [59]. SYBR® Green is a popular fluorescent dye, binding to the double stranded DNA non-specifically. By intercalating to the DNA, a fluorescent signal is emitted, therefor the increase of DNA during the PCR reaction leads to an increase in fluorescence and therefor magnification of the signal. An alternative to SYBR® Green is the utilization of so called TaqMan® Probes – hydrolysis probes that rely on Förster Resonance Energy Transfer. A probe usually consists of a short ssDNA with a reporter (5') and a quencher (3'), that blocks emission if it is close to a reporter. During the extension step by DNA polymerase, the TaqMan® Probe is then cleaved and the reporter is able to emit a signal (fluorescence). Due to their design hydrolysis probes reach higher specificity then dyes that bind to the double stranded DNA (e.g. SYBR® Green) [59].

RT-qPCR has gained importance due to its specificity, sensitivity and promptness, and it allows both – an absolute (standard curve) and a relative quantification (housekeeping genes). The success and performance of the reaction depends on primer design and reagents quality (and choice). The results and eventually analysis of gene expression can be influenced by all mentioned above.

The relative transcript abundance of the genes *dia1* to *dia5*, *diaR1* and *diaR2* were measured for the overexpression strain OEdiaR1 and the deletion strains listed in Table 5.1. In this study relative quantification was used, based on the comparison to the transcript abundance of the reference genes *sar1* and *act*. The housekeeping gene *sar1* encodes for a GTPase and was previously identified as a very stable gene, suitable as a reference gene for RT-qPCR [61]. Although throughout literature the expression stability of *act*, encoding for actin, has been criticized [62], for *Trichoderma* it has been established as a reliable reference gene [61].

Table 5.1.: Overexpressed and deleted strains utilized in the scope of this work and their designation

Strain	**Overexpressed/deleted gene**
OEdiaR1	Overexpression of *diaR1* (under constitutive TEF1 promotor)
Δdia1	Deletion of *dia1* (PKS)
Δdia2	Deletion of *dia2* (Lactamase like protein)
Δdia3	Deletion of *dia3* (Dehydrogenase)
Δdia4	Deletion of *dia4* (FAD dependent oxidoreductase)
Δdia5	Deletion of *dia5* (FDH-MT)

5.3. Objectives

The aim of this work is the construction of a *T. reesei* QM6a △mus53 deletion strain, whereby the gene *dia3* (encoding for a dehydrogenase) is targeted. Intended deletion should be achieved by a protoplast-mediated tarnsformation with a previously designed split marker system, using hygromycin as a split marker. Besides measuring the relative transcript abundance of the genes genes *dia1* to *dia5*, *diaR1* and *diaR2* for the overexpression strain OEdiaR1 and the deletion strains further comparison of the strains involves growth analysis by microscopy. Furthermore, dry cell weight, and thereby the biomass production, was compared for all deletion strains to the wild type.

6. Material & Methods

6.1. Media Preparation

All media required for the cultivation of *Trichoderma reesei* and generated deletion strains are listed in the table below with the exact composition given. Media was autoclaved and stored at room temperature until further required.

Table 6.1.: Recipes for required media for the cultivation of *Trichoderma reesei* and produced deletion strains

Medium	Composition
LB	1 % Peptoone, 1 % Sodium Chloride, 0.5 % Yeast Extract
MAM	For 1 L total amount of MA-Medium, 20 mL 50x Trace Elements, 250 mL 2x Mineral Salts, 500 mL 0.1 M Phosphate Citrate Buffer (pH 5), 1 mL 5 M Urea, 10 g Glycerol and 1 g Peptone were added and filled up to 1 L with ddH2O.
MEX	3 % Malt Extract, 0.1 % Peptone, 0.5 % Yeast Extract
	If required, 1.5 % Bacteriological Agar was added.

Table 6.2.: Recipe for Trace Elements, Mineral Salts and Phosphate Citrate Buffer for MAM

Medium	Composition
50x Trace Elements	0.9 mM $FeSO_4$·7 H_2O, 0.31 mM $MnSO_4$·H_2O, 0.24 mM $ZnSO_4$·7 H_2O, 0.77 mM $CoCl_2$·6 H_2O
2x Mineral Salts	43.8 mM $(NH_4)_2SO_4$, 58.32 mM KH_2PO_4, 4.86 mM $MgSO_4$·7 H_2O, 10.88 mM $CaCl_2$·2 H_2O
0.1 M Phosphate Citrate Buffer	For 1 L of 0.1 M Phosphate Citrate Buffer 17.8 g of Na_2HPO_4·2 H_2O are dissolved in water, pH is adjusted to 5 with citric acid and then filled up to 1 L with ddH_2O

6.2. Strains and Cultivation

The strain *Trichoderma reesei* QM6a △mus53 (Steiger *et al.*, 66) was used in this study. Unless stated otherwise, it was cultivated on MEX with 1.5 % Bacteriological Agar at 30 °C. If required, the medium was supplied with uridine to a final concentration of 5 mM, and/or 5-fluoroorotic acid (5-FOA) was added to a final concentration of 2 mg/mL. For liquid cultures, cultivation occurred in Mandels Andreotti Medium and the agitation speed was adjusted to 180 rpm.

6.3. Primer Design

All primers designed in the scope of this work, including their sequence, are listed in Table 6.3. Delivered lyophilized primers were prepared by adding nuclease-free water to a final concentration of 100 mM, according to the manufacturer's instructions. For PCR purposes, the primers were further diluted to 10 mM and stored at -20 °C.

Table 6.3.: Primer sequences used in the scope of this project (D781-D788)

Primer Nr.	Primer Name	Sequence
C179	PgpdA_fwd	GAGCTCTGTACAGTGACCGG
C180	hph_MR	CGTCAGGACATTGTTGGAGC
C181	hph_MF	GACCTGCCTGAAACCGAAC
C182	TtrpC_rev	AGGTCGAGTGGAGATGTGGAG
C818	5'_flank_dia3_fwd	GAACATGCATGGGCCAAC
C819	5'_flank_dia3_rev_hph	CCGGTCACTGTACAGAGCTCCCATTGTGTCAAGCCGTG
D820	3'_flank_dia3_fwd_hph	CTCCACATCTCCACTCGACCTTGCGTAAGAAGCTGGTATGAC
D821	3'_flank_dia3_rev	CCACCTGACTACTAATCTGCC

6.4. Construction of △dia3

To gain further insight into the *dia* BGC, a wild type (QM6a △mus53) deletion mutant was constructed, whereby the gene *dia3* was deleted.

For this purpose a split marker strategy was used, whereby in this study hygromycin (*hph* from pAN7 [63]) served as a marker. Two overlapping fragments were constructed, using Q5® polymerase and pAN7 as a template, and designated hph_N (primer C179 and C180) and hph_C (C181 and C182) (Figure 6.1).

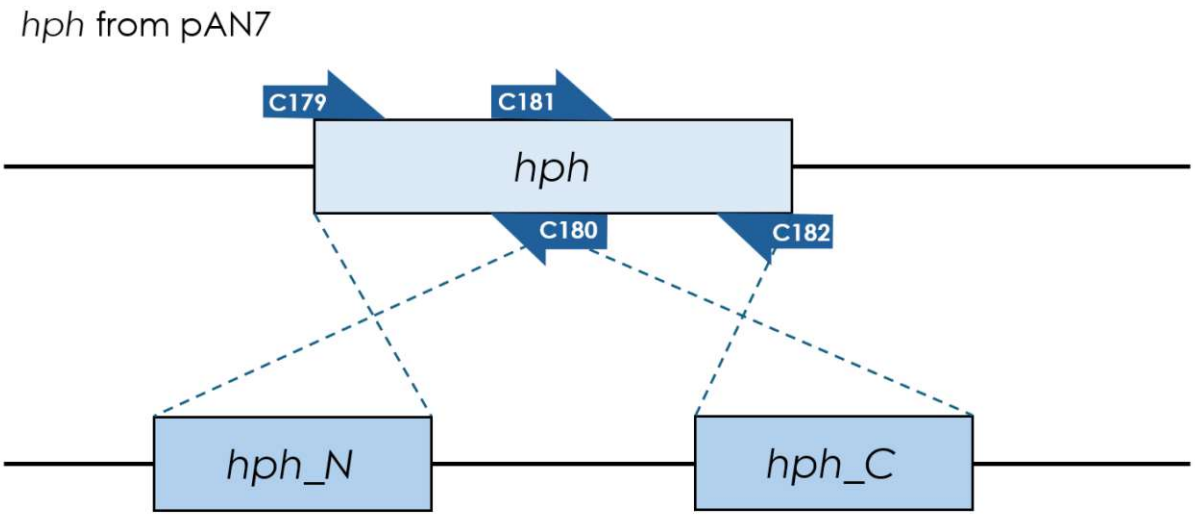

Figure 6.1.: Construction of overlapping fragments of hph (pAN7); hph_N was constructed using primers C189 and C180 and hph_C by using primers C181 and C182

In the following step a 5' and 3' flank were designed for the gene *dia3* (Figure 6.2,a) using primer C818 and C819 for the 5'_flank and C820 and C821 for the 3'_flank, followed by their fusion to *hph* overlapping hygromycin fragments. The fusion of the flanks and the overlapping fragments was performed by a SOE (Splicing by Overlap Extension) PCR using Q5® polymerase (reaction mixture and setup are given in Table 6.4 and Table 6.5), resulting in 5'_flank_hph_N (primer C180 and C818) and 3'_flank_hph_C (C181 and C821).

Table 6.4.: Required reagents for Q5® PCR

Reagent	Amount [µL]
Q5® Reaction Buffer	10
dNTPs	1
Forward Primer	2.5
Reverse Primer	2.5
Q5® Polymerase	0.5
Template (5ng/µL)	1
ddH_2O	32.5
$\sum$	50

Table 6.5.: Q5® PCR Cycler Condititions (according to manufacturer), whereby the steps denaturation, annealing and extension were repeated for 30 cycles

Step	Temperature [$^{\circ}C$]	Time [sec]
Initial Denaturation	98	120
Denaturation	98	8
Annealing	Individual for each primer	20
Extension	72	20-30 sec/kb
Final Extension	72	120
Hold	4	∞

The product yielded by the SOE PCR was directly transformed into *T. reesei* QM6a Δmus53. For successful transformation, overlapping of 5'_flank_hph_N and 3'_flank_hph_C is required. The overlap results in a hygromycin resistance (Figure 6.2,b), therefor transformants, in which the deletion of *dia3* did not occur, cannot survive on hygromycin containing selection media. Positive transformants were consequently confirmed by PCR.

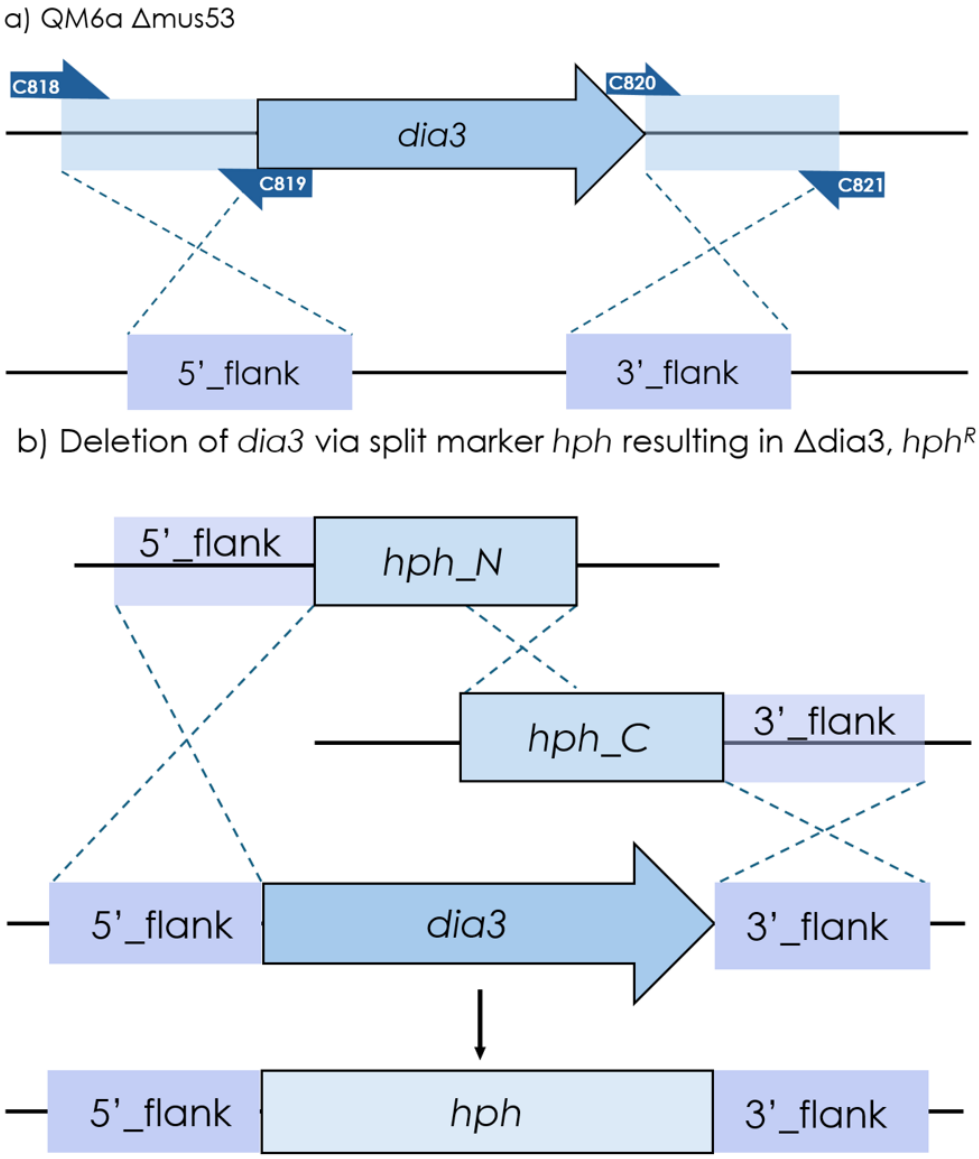

Figure 6.2.: a) Construction of 5' and 3' flank for their consequent fusion to *hph* fragments b) Schematic representation of successful deletion of *dia3* and insertion of a hygromycin resistance, assuming a correct crossover of constructed flanks

A 6x Loading Dye was introduced to each PCR product and the mixture was then loaded onto a 0.8 % agarose gel. Subsequently a gel electrophoresis was performed, adjusting the settings to 100 V and 45 minutes running time. For visualization of the gel the ChemiDoc™ Touch Imaging System was used. The targeted band was cut out and the DNA was purified with NEB Monarch® DNA Extraction Kit. Finally concentration was measured with NanoDrop One/One© UV/Vis Spectrophotometer.

6.5. Transformation via protoplasting

The first step of protoplast-mediated transformation is the preparation of all required media, which is listed in Table 6.6 [18][38].In addition 1.2 M Sorbitol was prepared. After the media was autoclaved buffer B and 1.2 M Sorbitol were stored at 4 °C, whereas buffer A and C, as well as the 60% PEG solution were stored at room temperature.

Table 6.6.: Required buffers for protoplast mediated transformation; after reagents are added buffers are filled up with ddH_2O until required volume is reached

Buffer	Reagents
Buffer A	100 mM KH_2PO_4 1,2 M Sorbit pH adjusted to 5.6 with KOH
Buffer B	1 M Sorbit 10 mM Tris.Cl (pH = 7.5) 25 mM $CaCl_2$
Buffer C	1 M Sorbit 10 mM Tris.Cl (pH = 7.5)
60 % PEG Solution (for a total volume of 100 mL)	60 g PEG 4000 1 mL 1 M Tris (pH = 7.5) 1 mL 1M $CaCl_2$ 38 mL ddH_2O Must be incubated at 50 °C in order to dissolve PEG.

On the first day, a *T. reesei* spore suspension was prepared and 100 µL of the suspension were transferred on a MEX plate covered with cellophane (previously autoclaved). The spores were distributed evenly on the plate with a Drigalski spatula and incubated overnight at 30 °C. In order to obtain enough mycelia for the transformation, three to four plates were prepared [18][38].

On the following day, the selection medium was autoclaved and stored at 55 °C until further needed. Lysing solution was prepared by dissolving 650 mg of Vinotaste (Novozymes, Denmark) in 15 mL of Buffer A. After stirring for approximately 10 minutes, the enzyme solution was

filtered through a 0.45 µm sterile syringe filter. The filtered solution was collected in a petri dish. Mycelia was scraped off the cellophane plates and transferred to the petri dish with the lysing solution, which was then incubated at 30 °C and 60 rpm for approximately three hours. Protoplasts were verified by a light microscope. After protoplasts were obtained, the solution was transferred to a 50 mL falcon and filled up to 40 mL with ice-cold 1.2 M sorbitol. After centrifugation at 2500 g/4 °C for 5 minutes, the supernatant was discarded, and the pellet was resuspended in 30 mL of ice-cold sorbitol. The centrifugation step was repeated, during which the sgRNA was loaded onto the Cas9. Therefore 15 µL 10x Cas9 Buffer, 4.25 µL EnGen Cas9 NLS, in total 2.7 µg sgRNA were mixed together and filled up to 150 µL with Buffer B, incubated for 10 minutes at 37 °C and stored on ice afterward. After centrifugation was completed, the supernatant was discarded, and the protoplasts pellet was very carefully resuspended in 1 mL of buffer B. Keeping the protoplasts on ice at all times and treating them carefully is crucial for a successful transformation. For each transformation reaction, a 50 mL falcon was cooled on ice. 150 µL of buffer B, DNA template, 100 µL protoplast solution, and 100 µL of 20 % PEG were mixed. After incubating the transformation mixture on ice for 30 minutes, 60 % PEG was added stepwise (50, 200, and 500 µL) and incubated for another 20 minutes at room temperature. Subsequently, buffer C was added stepwise (200, 400, 1000, and 2500 µL). Prior to plating, each falcon was filled up to 50 mL with the selection medium, warmed up to ca. 55 °C and poured onto a plate. The plates were then incubated for approximately 7 days under light at 30 °C [18][38].

Visible colonies were transferred to selection plates with added IGEPAL (Sigma Aldrich, Germany) to a final concentration of 1 mL/L (added prior autoclaving).

6.6. RNA Isolation and RT-qPCR

All strains (Table 5.1), as well as the wild type, were cultivated in Mandels Andreotti Medium for 72 h at 30 °C and 180 rpm. For the RNA extraction the mycelium was wrung in Miracloth Filtration Paper, in order to get rid of the medium residues, snap froze in liquid nitrogen and stored at -80 °C.

For RNA isolation the TriZol Zymo Reasearch Kit (Direct-zol™ RNA Miniprep Plus) was used, whereby 20 mg of mycelium were transferred to a screw cap reaction tube filled with glass

beads (0.37 g of 0.5 mm glass beads, 0.25 g of 1 mm glass beads and one large 5 mm glass bead) and 1 mL of TriZol Reagent®. The mycelium was then disrupted using the FastPrep-24™ Classic bead beating grinder and lysis system at level 6 for 30 seconds. After an incubation time of 5 minutes, a centrifugation step followed (5 minutes/12 000 g/RT). 700 µL of the aqueous phase were transferred to a new reaction tube (1.5 mL) and 700 µL of 0.96 % ethanol were added. After vortexing the mixture the Zymo-Spin™ IIICG Column was loaded (3x 500 µL) and centrifuged at 16 000 g/30 seconds/RT. After loading the column, 400 µL of RNA Wash Buffer was added, followed by centrifugation (16 000 g/ 30 seconds/ RT). 5 µL of DNase (6 U/µL) and 75 µL of DNA Digestion buffer were premixed, loaded on the column and incubated for 15 minutes. The column was then washed twice with 400 µL RNA Pre-Wash Buffer and centrifuged (16 000 g/ 30 seconds/ RT). Final washing step was performed by adding 700 µL of RNA Wash Buffer at 16 000 g for one minute at room temperature. The flow through is then discarded, centrifugation step repeated and RNA eluted by adding 30 µL of RNase-free water in a new reaction tube (1.5 mL). RNA concentration was measured using a NanoDrop Spectrophotometer.

Prior cDNA Synthesis RNA samples were diluted to a final concentration of 62.5 ng/µL (for easier handling). For cDNA synthesis LunaScript® RT SuperMix Kit (New England Biolabs ®) was used, therefore 2 µL of LunaScript® RT SuperMix were added to 8 µL of RNA (62.5 ng/µL). The RNA was then converted to cDNA using the BioRad Thermal Cycler T100 using the program given in Table 6.7 provided by the manufacturer.

Table 6.7.: Luna Script® RT SuperMix Kit Cycler Conditions according to manufacturer

Step	Temperature	Time
Primer Annealing	25 °C	60 sec
cDNA Synthesis	55 °C	10 min
Heat Inactivation	95 °C	60 sec
Hold	4 °C	∞

Finally the cDNA was diluted with ddH_2O 1:50. For the RT-qPCR Luna® Universal qPCR Master Mix was used, with a total reaction volume of 15 µL. The pipetting scheme is presented in Table 6.8.

Table 6.8.: RT-qPCR Luna® Universal qPCR Master Mix Pipetting Scheme

Reagent	Volume [µL]
Luna® Universal qPCR Master Mix	7.5
Primer Forward (10 µM)	0.375
Primer Reverse (10 µM)	0.375
ddH_2O	4.75
Template (cDNA)	2

The RT-qPCR was carried out using the Quiagen Rotor Gene Q Thermo Cycler (Quiagen, Netherlands) and the reaction conditions were provided by the manufacturer and are presented in Table 6.9.

Table 6.9.: Reaction conditions of Quiagen Rotor Gene Q Thermo Cycler, whereby denaturation and extension step were repeated for 40 to 45 cycles

Step	Temperature	Time
Initial Denaturation	95 °C	60 sec
Denaturation	95 °C	15 sec
Extension	60 °C	30 sec
Melt Curve	60 to 95 °C	varying

6.7. Evaluation of RT-qPCR

To obtain a deeper insight in the *dia* BGC in *T. reesei* and to activate the cluster, *diaR1*, encoding the zinc cluster protein, was previously overexpressed by positioning the coding region under the regulation of the TEF1 promotor, resulting in the overexpression strain designated OEdiaR1. Furthermore OEdiaR1 deletion mutants were constructed (see Table 5.1), in order to analyse the strains by means of RT-qPCR. For the relative quantification and within the evaluation of the gene expression levels, a mathematical model was published in 2001 by Pfaffl *et al.* [64], which takes the reference genes, the target gene, and their efficiency into consideration. The used formula established by Pfaffl *et al.* [64] and used for the analysis of the RT-qPCR results is given below (Equation (6.1)).

$$ratio = \frac{(E_{\text{target}})^{\Delta Ct_{\text{target(control-sample)}}}}{(E_{\text{ref}})^{\Delta Ct_{\text{ref(control-sample)}}}} \tag{6.1}$$

This model delivers a numeric value, so called ratio, of the target gene relative to the reference gene. Both variables E_{target} and E_{ref} refer to the efficiency of the PCR amplification, whereby E_{target} stands for the efficiency of the gene of interest and E_{ref} is the efficiency of the reference gene. The difference in the cycle threshold, ΔCt, between the sample and the control, which is the wildtype (in this case QM6a Δ mus53) for the target gene and the reference genes, reveal the changes in gene expression. A ΔCt_{ref} value, that equals 0 (or approximately 0) is a good indicator for a stable housekeeping gene, since it is not expected to be up- or downregulated nor fluctuating throughout different conditions.

6.8. Microscopy

The wild type QM6a ∆mus53 and all deletion strains were cultivated for 72 h in Mandels Andreotti Medium at 30 °C and 180 rpm (in quadruplicates). Samples were then taken, previously ensuring homogeneity by shaking the flasks, placed on a microscope slide and covered with a cover glass. Photographs were taken using a light microscope (NIKON ECLIPSE E200) provided with a BRESSER MikrOkular Okularkamera (Full HD), by varying magnifications, however in the scope of this work the images at a magnification of 40x were used for the analysis.

6.9. Dry Cell Weight (DCW) Measurement

For measurement of the dry cell weight the wild type QM6a ∆mus53 and all deletion strains were first cultivated for 72 h in Mandels Andreotti Medium at 30 ℃ and 180 rpm (in quadruplicates). The mycelium of each strain was then filtered through Miracloth Filtration Paper, which was previously weighed on an analytical balance (quadruplicates of each strain were filtered together through one filtration paper). The mycelium (with the paper) was then dried for 24 h at 80 °C. Consequently the weight of the dried mycelium was measured and compared for each strain.

7. Results

7.1. Construction of $\triangle$dia3

In Figure 7.1 the bands of 5'_flank_dia3 at 403 bp, 3'_flank_dia3 at 347 bp, and both hph fragment, hph_N (1489 bp) and hph_C (1513 bp) are visible. For hph_N the bands at 1489 bp are only slightly visible, therefore the PCR was repeated at a higher temperature (67 °C).

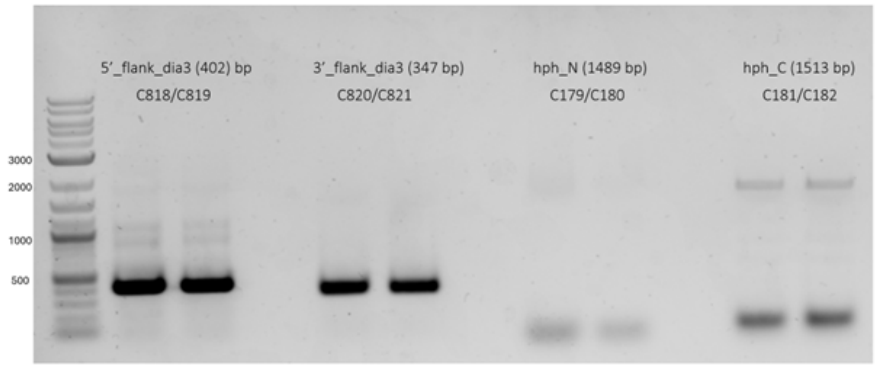

Figure 7.1.: Constructed flanks for *dia3* (approximately at 300 bp) and hph (approximately at 1500 bp)

The SOE PCR yielded in the products 5'_flank_hph_N and 3'_flank_hph_C, which are shown in Figure 7.2. The band of 5'_flank_hph_N is located at 1900 bp and the band of 3'_flank_hph_C is to be found at 1860 bp.

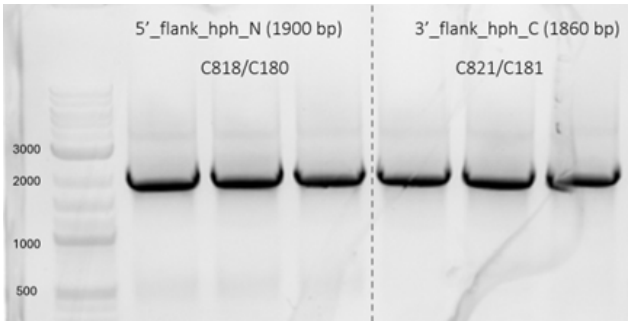

Figure 7.2.: 5'_flank_hph_N (at 1900 bp) and 3'_flank_hph_C (at 1860 bp)

The obtained purified product was directly used in the fungal transformation. Eventually DNA was extracted of potentially positive deletion mutants and used for the PCR, in order to confirm if deletion of *dia3* was successful. As negative control water was added instead of DNA. The used primers are summarized in Table 7.1 and the loaded PCR product visualized on a gel in Figure 7.3. Furthermore, in order to show where the primers bind, a schematic visualization is given in Figure 7.4.

Table 7.1.: Samples and used template (DNA template in columns a - c) for the confirmation of positive deletion of *dia3*

Nr.	a	b	c	Primer
1	NC (H_2O)	OEDiaR1	Δdia3	C991/C992
2	NC (H_2O)	OEDiaR1	Δdia3	C991/C180
3	NC (H_2O)	OEDiaR1	Δdia3	C992/C181

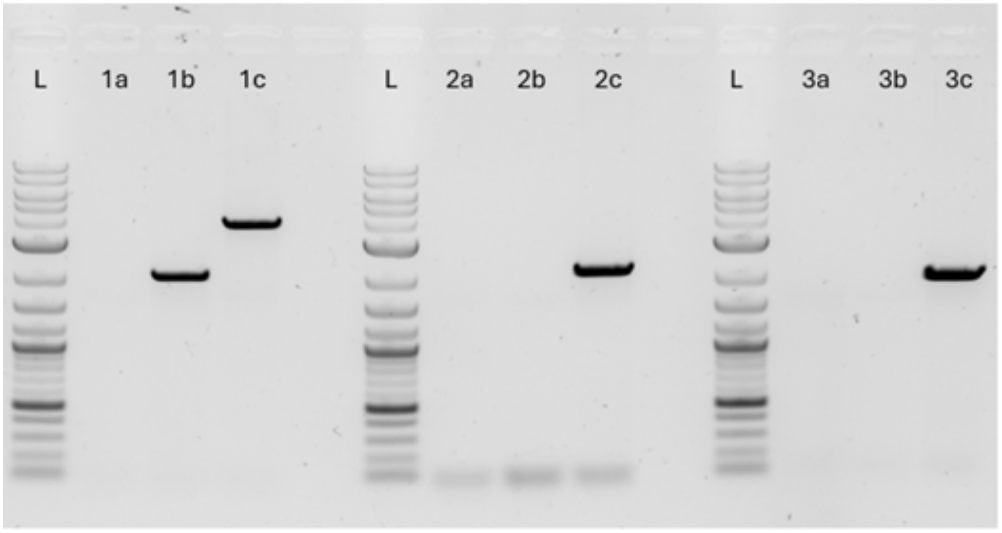

Figure 7.3.: Confirmation of positive deletion of *dia3*

For reactions 1a to 3a, instead of DNA, water was added, thus no visible bands were expected. This was successfully confirmed and is shown in Figure 7.3. In the PCR reaction 1b the primers C991 and C992 were applied, whereas the OEDiaR1 served as a template. In this case the gene *dia3* is not deleted, hence the primer bind at the beginning of the 5' flank and at the end

of the 3' flank, resulting in a band (approximately 2000 bp). The band visible for reaction 1c (at approximately 4000 bp) is indicating a successful integration of the *hph* gene, whereby an overlap of 5'_flank_hph_N and 3'_flank_hph_C is a prerequisite. Reactions 2b and 3b do not yield in a product, since the primers C180 and C181 are designed to bind directly to *hph*. However, since in the strain OEDiaR1 this gene is absent the primers cannot bind. On the contrary the successful overlap of 5'_flank_hph_N and 3'_flank_hph_C and the binding of primers C180 and C181 indicate the deletion of *dia3* and intergration of *hph* (shown in Figure 7.4.

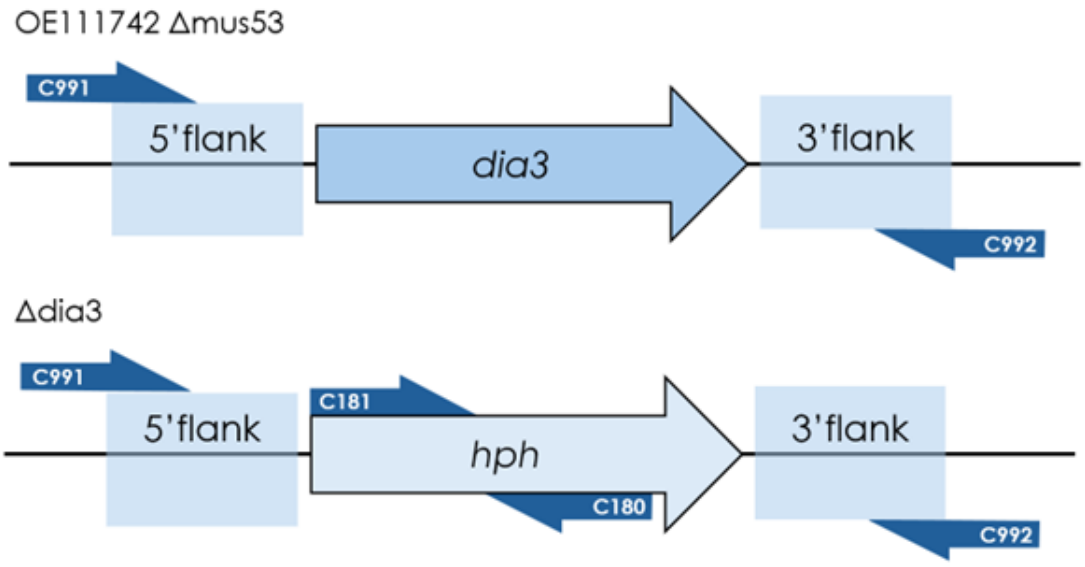

Figure 7.4.: Schematic representation of the genes *ura3* and *hph* and the position of primer binding

7.2. Comparison of *dia* strains via RT-qPCR

The RT-qPCR results are presented in Figure 7.5.. The values for the relative transcript abundance, which are placed on the y-axis, were logarithmized in order to underline and enhance the differences between the strains. On the horizontal axis the genes *dia1* to *dia5*, *diaR1* and *diaR2* are given. Additionally the wildtype QM6a Δ mus53 was analyzed and it is clearly visible that, as expected, the genes are not upregulated, indicating that the *dia* BGC is not active, if *diaR1* is not activated. On the other hand when *diaR1* is overexpressed, all targeted genes of the BGC are upregulated. Furthermore the analysis shows that the deletion for each gene was successful, since the relative transcript abundance of the deleted gene is approximately zero.

It is noticeable that the deletion of *dia1* does not affect the transcript abundance of the other genes significantly. On the other hand, when the rest of the genes of the *dia* BGC are deleted, it can be observed that *dia1* is slightly downregulated. The lowest transcript abundance values were observed, when *dia3* is deleted, however throughout the deletion strains, the transcript abundances levels are steady.

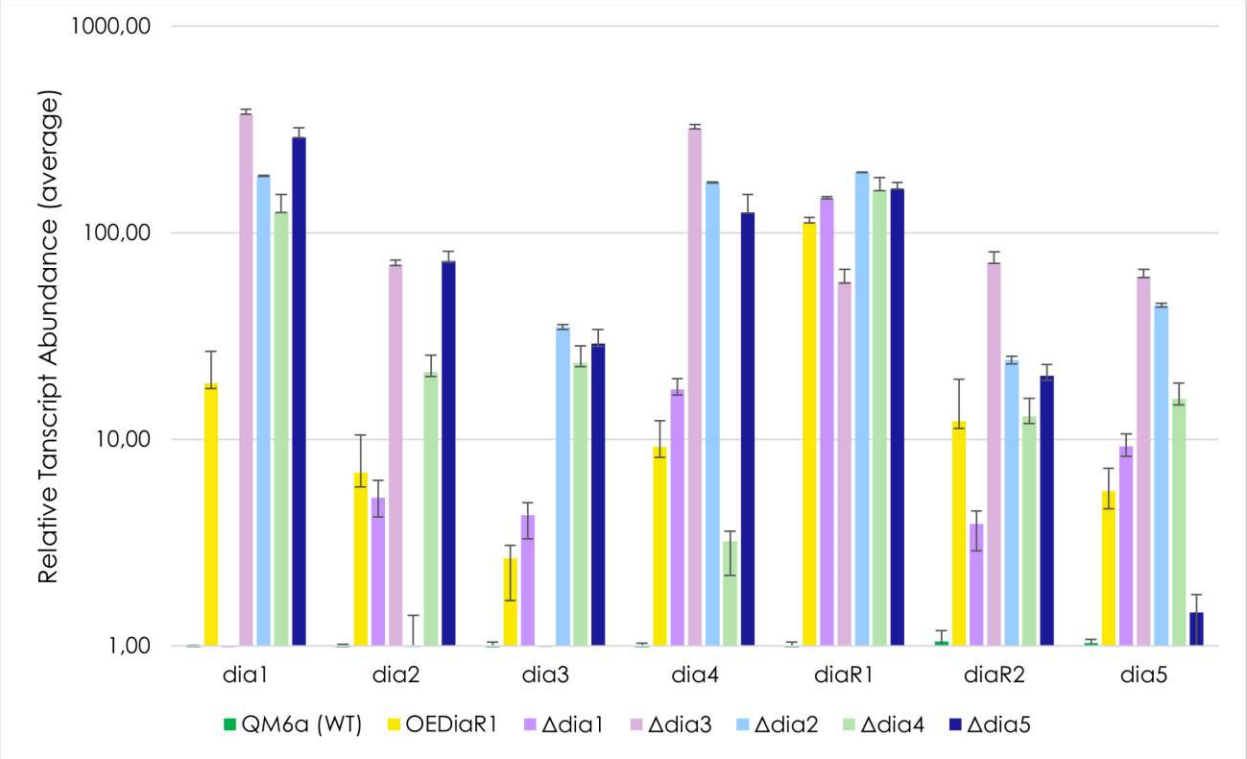

Figure 7.5.: RT-qPCR results evaluated by means of equation 6.1

7.3. Comparison of *dia* strains via microscopy

After an incubation time of 72 h photographs of the strains were captured, to indicate the visible (with the naked eye) difference between each strain compared to the wild type. Furthermore, microscopic images at a magnification of 40x were used for further comparison.

The photos of the wild type QM6a Δmus53, the overexpression strain and Δdia3 are shown in Figures 7.6 to 7.9. In comparison to the wild type, which seems to grow thick and elongated hyphae, the growth of the overexpression strain seems to be slightly disrupted, since the hyphae are not as strongly presented as in the wild type.Through the rotation movement in the shaker the hyphae are glued down to the wall of the flask, leading to agglomeration of the mycelium, and in contrast to the overexpression strain there are no single colonies visible. The strain Δdia3 behaves differently, since its growth seems to be significantly impaired by the deletion of the gene *dia3*.

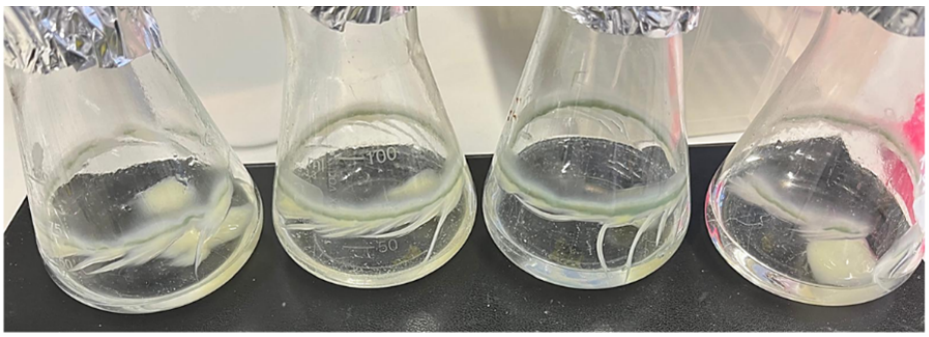

Figure 7.6.: Wild Type in MAM after incubation for 72 h; is characterized by thick and elongated branched hyphae, as well as visible septa; on the right side an agglomeration of spores is visible

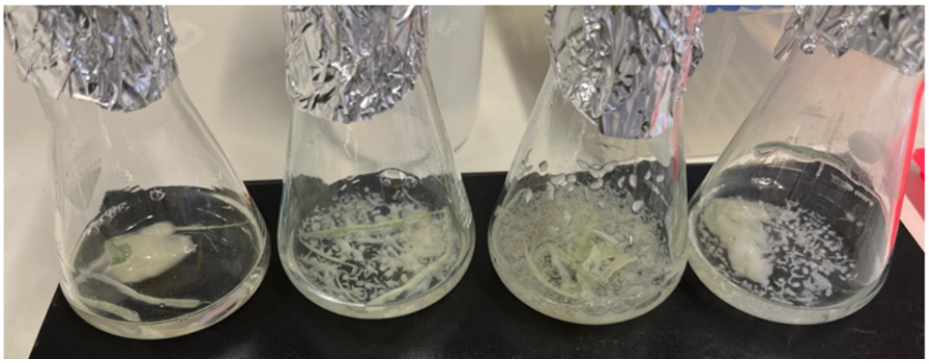

Figure 7.7.: OEdiaR1 in MAM after incubation for 72 h;slightly thinner hyphae compared to the WT; however features are strongly comparable to the wild type

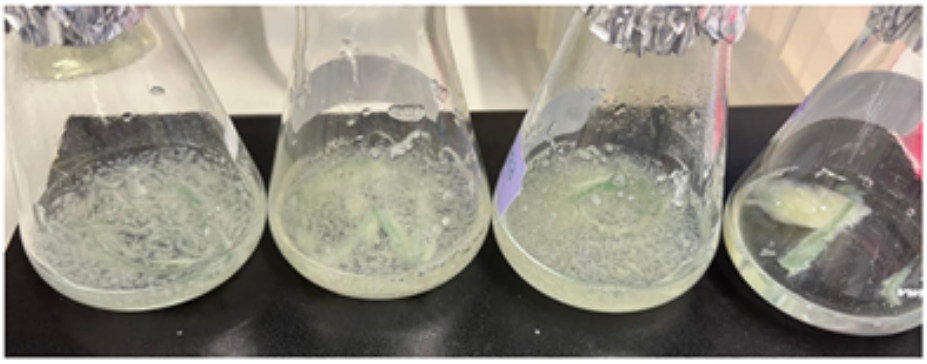

Figure 7.8.: Δdia3 in MAM after incubation for 72 h; characterized by thin hyphal growth and less spores were observed

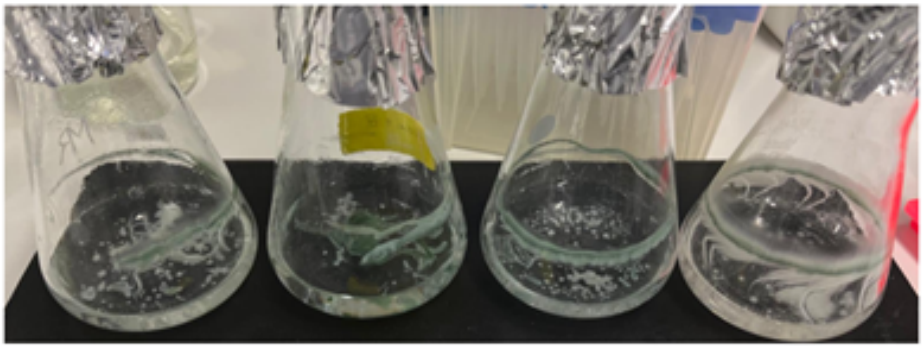

Figure 7.9.: Δdia1 in MAM after incubation for 72 h; similar behaviour to the *dia3* deletion strain

When the microscopy photos are taken into consideration, it can be observed that for the wild type the hyphae are highly branched and the septa are clearly visible. In addition a lot of spores, with thick walls can be found (Figure 7.10). The overexpression strain shows a similar behavior to the wild type and cannot be distinguished under the microscope with certainity (Figure 7.11). When Δdia3 is observed under the light microscope it is noticeable, that the hyphae appear thinner than in the wild type and overexpression strain, which could be a further indicator for growth impairment (Figure 7.12). Furthermore, the total number of the spores, even though the strains underwent the same conditions, is lower. Under the microscope the same behavior was observed for Δdia1 (Figure 7.13).

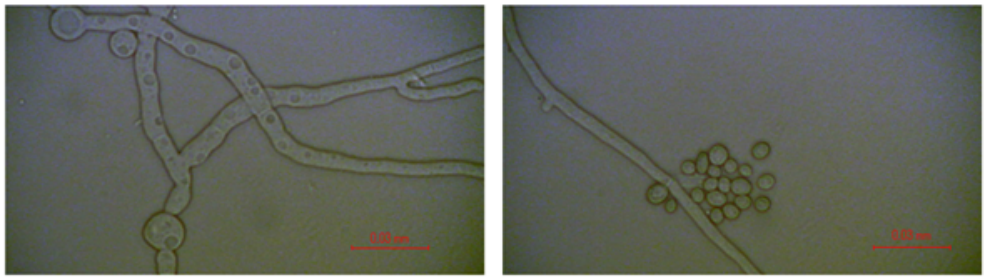

Figure 7.10.: Wild Type under the light microscope at a magnification of 40x

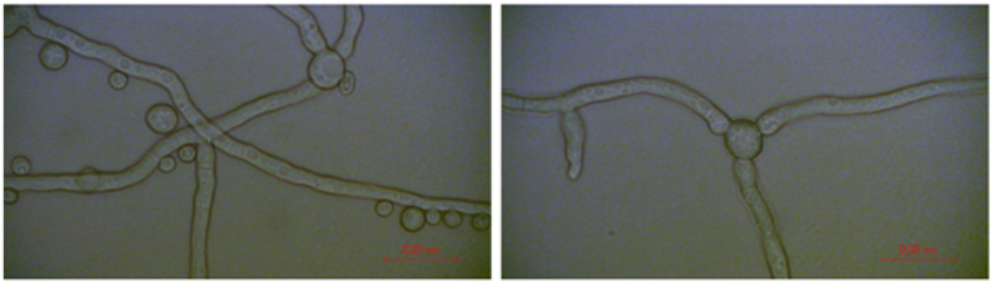

Figure 7.11.: OEdiaR1 under the light microscope at a magnification of 40x

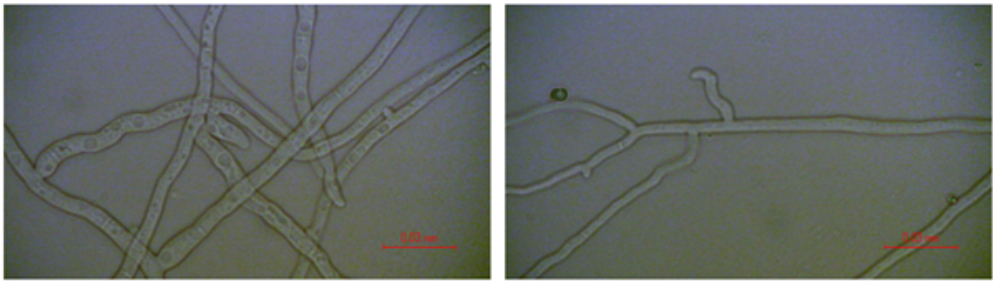

Figure 7.12.: Δdia3 under the light microscope at a magnification of 40x

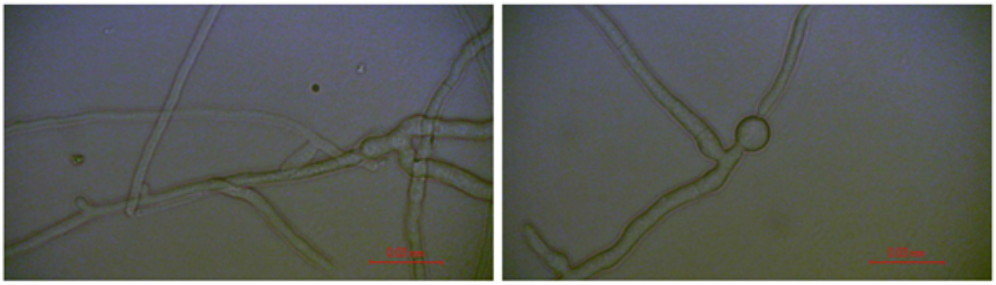

Figure 7.13.: Δdia1 under the light microscope at a magnification of 40x

7.4. Comparison of Cell Dry Weight (DCW) of *dia* strains

After the mycelium was dried at 80 °C for 24 hours, the biomass was measured at a analytical balance. The results are summarized in Figure 7.14. In correlation to previous findings (microscopy and visual analysis, Section 7.3), the deletion strain Δdia3 is characterized by the lowest biomass production (0.05 g). Compared to wild type QM6a Δmus53 (0.29 g) and OEdiaR1 (0.32 g), this is a decrease of biomass production by a factor of six for Δdia3. For the strains Δdia1 (0.19 g), Δdia2 (0.20 g), Δdia4 (0.16 g) and Δdia5 (0.13 g) the biomass production is lower in comparison to the wild type and the overexpression strain, but not as low as the strain Δdia3. Furthermore, it can be observed that the WT Δdia3 exhibits the highest cell dry weight of all strains (0.38 g).

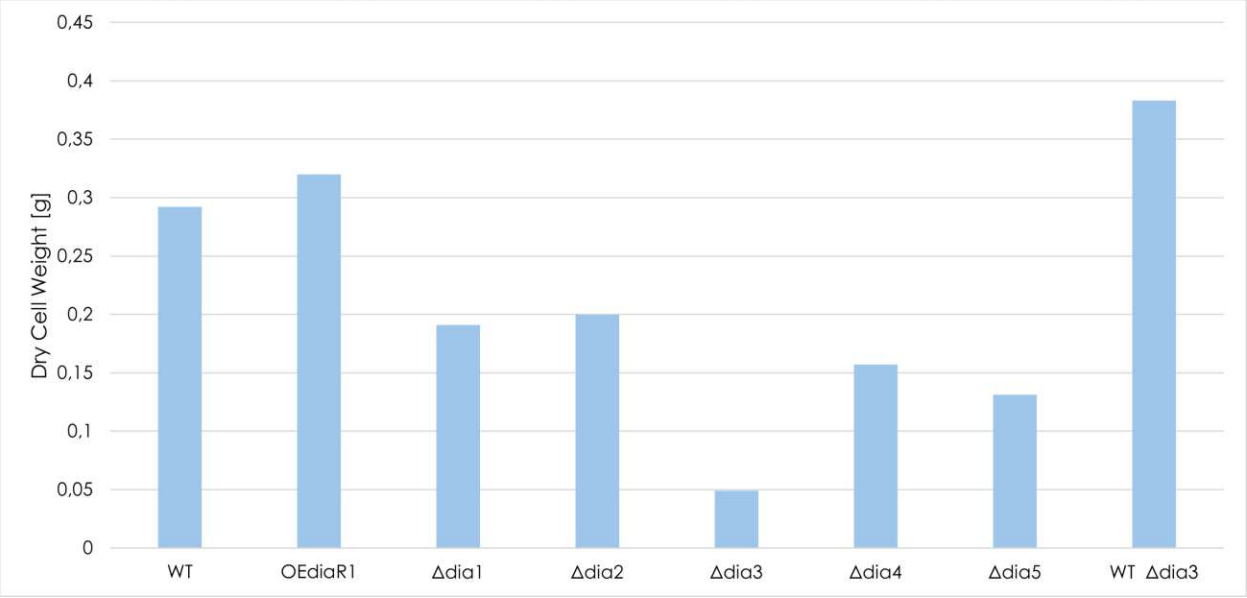

Figure 7.14.: CDW results obtained for all strains after 24 h at 80 °C

8. Discussion

In the scope of this work a deletion of the gene *dia3* was successfully achieved in the *T. reesei* strain QM6a ∆mus53 via protoplast-mediated transformation. In addition the produced mutant was compared to other deletion strains (∆dia1, ∆dia2, ∆dia3, ∆dia4, ∆dia5) and to the overexpression strain OEdiaR1, regarding gene expression, whereby the house-keeping genes *sar1* and *act1* were applied as reference genes. Additionally, the growth of all strains was closely analysed by microscopy and by comparison of the obtained cell dry weight.

These findings contributed to the extended research of the *dia* biosynthetic gene cluster and its role in the production of diaporthinic acid, which was previously suspected to possess antimicrobial properties. These results are further discussed in the paper "*In vivo activation of the* dia *BGC allows consolidation of the biosynthetic pathways of diaporthin, dichlorodiaporthin, diaporthinic acid, and diaporthinol*" [65], a study I was allowed to contribute to with the construction of the deletion strain QM6a ∆mus53 ∆dia3 and by analysis of the trascript abundance levels via RT-qPCR of the wild type QM6a ∆mus53, over expression strain OEDiaR1 and all deletion strains .

Gene expression analysis revealed that deletion of the gene *dia3* resulted in the lowest transcript abundance values, thus corresponding to the findings in Section 7.3., in which it is apparent that the deletion strain ∆dia3 has an impaired growth. However throughout the deletion strains, the transcript abundances levels are steady and similar to the transcript abundance levels of the overexpression strain. Summed up, this could indicate the significance of *dia3* in the *dia* BGC, which encodes for a dehydrogenase.

When the strains are visually compared, it is noticeable that the over expression strain OEdiaR1 grows differently from the wild type, indicating growth inhibition due to the activation of the *dia* BGC. It has been discovered that secondary metabolites resulting from the *dia* BGC, such as dichlorodiaporthin and diaporthinol, often have significant antifungal activities [66], which consequently would explain the induced growth inhibition. Based on further findings, obtained by Burger et al. in the previously mentioned publication [65], we were able to discover that

the deletion of the gene *dia3* is connected to the accumulation of the biosynthetic products dichlorodiaporthin, diaporthinic acid, citreoisocoumarin and 6-methyl-citreoisocoumarin. Compared to the overexpression strain (OEdiaR1), those metabolites are expressed in much higher amounts. Secondary metabolites accompanied by antifungal activity [67], reinforces the theory that the deletion strain Δdia3 might underlie growth inhibition.

Deletion of *dia1*, that encodes for a polyketide synthase (PKS), showed similar growth behavior to the wild type, which correlates to the RT-qPCR results, however two out of four quadruplicates, seem to be impaired in their growth to a small extend. Furthermore, under the light microscope (Section 7.3.) a slight decrease of thickness of the hyphal and spore cell wall was noticeable.

A study published in 2021 by Meng *et al.* [68], discovered that the deletion of a polyketide synthase (pks11) in *Beauveria bassiana* is connected to decrease of thickness of the cell wall of spores, which might underline the importance of polyketide synthases in spores germination. Furthermore, Atanasova *et al.* [69], studied the role of genes encoding for polyketide synthases in *T. reesei*, focusing on *pks4*, highlighting its importance in conidial pigmentation and the stability of the cell wall. Deletion of *pks4* resulted in the decrease of mechanical stability when exposed to increased air pressure [69]. These findings align with the results obtained in the scope of this work, however the diversity of polyketides does not allow for us to draw direct conclusions. The exact structure of the polyketide is necessary for a direct comparison - enabling a further research point.

However it seems that the growth impairment introduced by the overexpression of *diaR1* is consequently abolished by the further deletion of *dia1*, since the relative transcript abundance of the genes of the *dia* BGC in the deletion strain Δdia1 is relatively high in comparison to the rest of the deletion strains.

Burger *et al.* [65] isolated diaporthinic acid as the main compound of the activated *dia BGC* and furthermore suggested that *dia1*, *dia2* and *dia5* are crucial for the production of diaporthinic acid, since their deletion resulted in the absence of diaporthinic acid. In addition the deletion of *dia5* (encoding for the bifunctional enzyme FDH-MT) results in the absence of dichlorodiaporthin, which consequently leads to abortion of the diaporthinic acid production.

At this point it is important to mention, that in this study, the transcript analysis was based on the housekeeping genes *sar1* and *act1*. Recently published study by Danner *et al.* [70], however refute the stability of these genes as reference genes. Considering this, the data obtained by the RT-qPCR must be viewed with caution. At the time of conducting the experiments those housekeeping genes were, to my knowledge, at the forefront of research and thereby reliable for the relative quantification. To obtain accurate results, this experiment should be repeated with stable housekeeping genes, for instance, as suggested by Danner *et al.* [70], the genes *tpc1* and *bzp1*.

The analysis of the dry cell weight highlights the growth inhibition of Δdia3, since this deletion strain produced approximately one sixth of the biomass compared to the wild type QM6a Δmus53 and the overexpression strain OEdiaR1. However it must be emphasized that, that the CDW analysis was performed in quadruplicates, but those were filtered together and therefor the obtained results serve solely for observation purposes. In order to obtain accurate results, the dry cell weight analysis should be repeated (in quadruplicates, filtered separately) and a standard deviation should be calculated, allowing an accurate conclusion.

Bibliography

[1] Jumbam, B et al. “A taxonomic revision of Aureobasidium (Saccotheciaceae, Dothideales) with new species, new names, and typifications”. In: *Persoonia-Molecular Phylogeny and Evolution of Fungi* (2024).

[2] Bridge Cooke, W. “AN ecological life history of Aureobasidium pullulans (De Bary) Arnaud”. In: (1906).

[3] Nieuwenhuijzen, E.J. van. “Aureobasidium”. In: (2014), pp. 105–109. DOI: 10.1016/b978-0-12-384730-0.00017-3.

[4] Gunde-Cimerman, Nina et al. “Hypersaline waters in salterns–natural ecological niches for halophilic black yeasts”. In: *FEMS microbiology Ecology* 32.3 (2000), pp. 235–240.

[5] Prasongsuk, Sehanat et al. “The current status of Aureobasidium pullulans in biotechnology”. In: *Folia Microbiologica* 63.2 (Oct. 2017), pp. 129–140. ISSN: 1874-9356. DOI: 10.1007/s12223-017-0561-4.

[6] Zalar, P. et al. “Redefinition of Aureobasidium pullulans and its varieties”. In: *Studies in Mycology* 61.NL-3508 (2008), pp. 21–38. ISSN: 0166-0616. DOI: 10.3114/sim.2008.61.02.

[7] Wang, Meizhu et al. “Comparative pathogenicity of opportunistic black yeasts in Aureobasidium”. In: *Mycoses* 62.9 (July 2019), pp. 803–811. ISSN: 1439-0507. DOI: 10.1111/myc.12931.

[8] Gostinčar, Cene et al. “Fifty Aureobasidium pullulans genomes reveal a recombining polyextremotolerant generalist”. In: *Environmental microbiology* 21.10 (2019), pp. 3638–3652.

[9] Zhdanova, Nelli N et al. “Fungi from Chernobyl: mycobiota of the inner regions of the containment structures of the damaged nuclear reactor”. In: *Mycological Research* 104.12 (2000), pp. 1421–1426.

[10] Rayner, ADM, Griffith, GS, and Ainsworth, AM. “Mycelial interconnectedness”. In: *The growing fungus*. Springer, 1995, pp. 21–40.

[11] Slepecky, Ralph A and Starmer, William T. “Phenotypic plasticity in fungi: a review with observations on Aureobasidium pullulans”. In: *Mycologia* 101.6 (2009), pp. 823–832.

[12] Smith, Daniel F. Q. and Casadevall, Arturo. “The Role of Melanin in Fungal Pathogenesis for Animal Hosts”. In: (2019), pp. 1–30. ISSN: 2196-9965. DOI: 10.1007/82_2019_173.

[13] Chi, Zhe et al. “The signaling pathways involved in metabolic regulation and stress responses of the yeast-like fungi Aureobasidium spp.” In: *Biotechnology Advances* 55 (2022), p. 107898.

[14] Wirshing, Alison C.E., Petrucco, Claudia A., and Lew, Daniel J. “Chemical transformation of the multibudding yeast, Aureobasidium pullulans”. In: *Journal of Cell Biology* 223.10 (June 2024). ISSN: 1540-8140. DOI: 10.1083/jcb.202402114.

[15] Rensink, Stephanie et al. “Use of Aureobasidium in a sustainable economy”. In: *Applied Microbiology and Biotechnology* 108.1 (2024), p. 202.

[16] Wang, Duoduo et al. “Advances and Challenges in CRISPR/Cas-Based Fungal Genome Engineering for Secondary Metabolite Production: A Review”. In: *Journal of Fungi* 9.3 (Mar. 15, 2023), p. 362. ISSN: 2309-608X. DOI: 10.3390/jof9030362.

[17] Li, Dandan et al. “Methods for genetic transformation of filamentous fungi”. In: *Microbial Cell Factories* 16.1 (Oct. 2017). ISSN: 1475-2859. DOI: 10.1186/s12934-017-0785-7.

[18] Kreuter, Johanna et al. “Fast and efficient CRISPR-mediated genome editing in Aureobasidium using Cas9 ribonucleoproteins”. In: *Journal of Biotechnology* 350 (2022), pp. 11–16.

[19] Gupta, Darshana et al. “CRISPR-Cas9 system: A new-fangled dawn in gene editing”. In: *Life Sciences* 232 (July 8, 2019), p. 116636. ISSN: 0024-3205. DOI: 10.1016/j.lfs.2019.116636.

[20] Huang, M and Graves, LM. “De novo synthesis of pyrimidine nucleotides; emerging interfaces with signal transduction pathways”. In: *Cellular and Molecular Life Sciences CMLS* 60.2 (2003), pp. 321–336.

[21] Jones, Mary Ellen. “Pyrimidine nucleotide biosynthesis in animals: genes, enzymes, and regulation of UMP biosynthesis”. In: *Annual review of biochemistry* 49.1 (1980), pp. 253–279.

[22] O’Donovan, Gerard A and Neuhard, Jan. “Pyrimidine metabolism in microorganisms”. In: *Bacteriological reviews* 34.3 (1970), pp. 278–343.

[23] Gruber, F et al. “The development of a heterologous transformation system for the cellulolytic fungus Trichoderma reesei based on a pyrG-negative mutant strain”. In: *Current genetics* 18.1 (1990), pp. 71–76.

[24] Santoso, Djoko. *5-Fluoroorotic acid-selected cell lines and regulation of UMP synthase gene expression in tobacco cells*. Iowa State University, 1995.

[25] Boeke, Jef D, La Croute, Francois, and Fink, Gerald R. “A positive selection for mutants lacking orotidine-5-phosphate decarboxylase activity in yeast: 5-fluoro-orotic acid resistance”. In: *Molecular and General Genetics MGG* 197.2 (1984), pp. 345–346.

[26] Ranjha, Lepakshi, Howard, Sean M, and Cejka, Petr. “Main steps in DNA double-strand break repair: an introduction to homologous recombination and related processes”. In: *Chromosoma* 127.2 (2018), pp. 187–214.

[27] Xue, Chaoyou and Greene, Eric C. “DNA repair pathway choices in CRISPR-Cas9-mediated genome editing”. In: *Trends in Genetics* 37.7 (2021), pp. 639–656.

[28] Ensminger, Michael and Löbrich, Markus. “One end to rule them all: Non-homologous end-joining and homologous recombination at DNA double-strand breaks”. In: *The British journal of radiology* 93.1115 (2020), p. 20191054.

[29] Ito, Yoichiro et al. “Deletion of DNA ligase IV homolog confers higher gene targeting efficiency on homologous recombination in Komagataella phaffii”. In: *FEMS yeast research* 18.7 (2018), foy074.

[30] Gostimskaya, Irina. “CRISPR–cas9: A history of its discovery and ethical considerations of its use in genome editing”. In: *Biochemistry (Moscow)* 87.8 (2022), pp. 777–788.

[31] Jansen, Ruud et al. “Identification of genes that are associated with DNA repeats in prokaryotes”. In: *Molecular microbiology* 43.6 (2002), pp. 1565–1575.

[32] Doudna, Jennifer A. and Charpentier, Emmanuelle. “The new frontier of genome engineering with CRISPR-Cas9”. In: *Science* 346.6213 (Nov. 25, 2014). ISSN: 1095-9203. DOI: 10.1126/science.1258096.

[33] Khurana, Amit et al. “A comprehensive overview of CRISPR/Cas 9 technology and application thereof in drug discovery”. In: *Journal of cellular biochemistry* 123.10 (2022), pp. 1674–1698.

[34] Lau, Cia-Hin, Tin, Chung, and Suh, Yousin. “CRISPR-based strategies for targeted transgene knock-in and gene correction”. In: *Faculty Reviews* 9 (2020), p. 20.

[35] Gostinčar, Cene et al. “Genome sequencing of four Aureobasidium pullulans varieties: biotechnological potential, stress tolerance, and description of new species”. In: *BMC Genomics* 15.1 (July 2014), p. 549. ISSN: 1471-2164. DOI: 10.1186/1471-2164-15-549.

[36] Nakata, Yasuhiko, Tang, Xiaoren, and Yokoyama, Kazunari K. “Preparation of competent cells for high-efficiency plasmid transformation of Escherichia coli”. In: *cDNA Library Protocols*. Springer, 1997, pp. 129–137.

[37] Davis, Leonard. *Basic methods in molecular biology*. Elsevier, 2012.

[38] Schmal, Matthias et al. “Providing a toolbox for genomic engineering of Trichoderma aggressivum”. In: *Microbiology Spectrum* (2025), e00966–25.

[39] D’Orio, Eugenio et al. “Troubleshooting and challenges of Next-generation sequencing technology in forensic use”. In: *Next Generation Sequencing (NGS) Technology in DNA Analysis*. Elsevier, 2024, pp. 471–484.

[40] Ramsden, Simon C et al. *Practice guidelines for Sanger Sequencing Analysis and Interpretation*. 2016.

[41] Maquat, Lynne E. “The power of point mutations”. In: *Nature genetics* 27.1 (2001), pp. 5–6.

[42] Poole, Leslie B. “The basics of thiols and cysteines in redox biology and chemistry”. In: *Free Radical Biology and Medicine* 80 (2015), pp. 148–157.

[43] Velíšek, Jan, Cejpek, Karel, et al. “Biosynthesis of food constituents amino acids 2. The alanine-valine-leucine, serine-cysteine-glycine, and aromatic and heterocyclic amino acids groups: a review.” In: *Czech Journal of Food Sciences* 24.2 (2006), pp. 45–58.

[44] Brosnan, John T and Brosnan, Margaret E. “The sulfur-containing amino acids: an overview”. In: *The Journal of nutrition* 136.6 (2006), 1636S–1640S.

[45] Allen, Felicity et al. “Predicting the mutations generated by repair of Cas9-induced double-strand breaks”. In: *Nature biotechnology* 37.1 (2019), pp. 64–72.

[46] Klim, Joanna, Zielenkiewicz, Urszula, and Kaczanowski, Szymon. “Loss-of-function mutations are main drivers of adaptations during short-term evolution”. In: *Scientific reports* 14.1 (2024), p. 7128.

[47] Hahm, Ja Young et al. “8-Oxoguanine: from oxidative damage to epigenetic and epitranscriptional modification”. In: *Experimental & molecular medicine* 54.10 (2022), pp. 1626–1642.

[48] Masi, Audrey et al. “Genomic deletions in Aureobasidium pullulans by an AMA1 plasmid for gRNA and CRISPR/Cas9 expression”. In: *Fungal Biology and Biotechnology* 11.1 (June 2024). ISSN: 2054-3085. DOI: 10.1186/s40694-024-00175-4.

[49] Galhardo, Rodrigo S, Hastings, Philip J, and Rosenberg, Susan M. “Mutation as a stress response and the regulation of evolvability”. In: *Critical reviews in biochemistry and molecular biology* 42.5 (2007), pp. 399–435.

[50] Mach-Aigner, Astrid R., Martzy, Roland, and Editors. “Methods in Molecular Biology”. In: (2234).

[51] Bischof, Robert H., Ramoni, Jonas, and Seiboth, Bernhard. “Cellulases and beyond: the first 70 years of the enzyme producer Trichoderma reesei”. In: *Microbial Cell Factories* 15.1 (June 2016). ISSN: 1475-2859. DOI: 10.1186/s12934-016-0507-6.

[52] Keshavarz, Behnam and Khalesi, Mohammadreza. “Trichoderma reesei, a superior cellulase source for industrial applications”. In: *Biofuels* 7.6 (June 2016), pp. 713–721. ISSN: 1759-7277. DOI: 10.1080/17597269.2016.1192444.

[53] Paloheimo, Marja et al. “Production of Industrial Enzymes in Trichoderma reesei”. In: (2016), pp. 23–57. ISSN: 2198-7785. DOI: 10.1007/978-3-319-27951-0_2.

[54] Gaynes, Robert. “The discovery of penicillin—new insights after more than 75 years of clinical use”. In: *Emerging infectious diseases* 23.5 (2017), p. 849.

[55] Ahuja, Manmeet et al. “Illuminating the Diversity of Aromatic Polyketide Synthases in Aspergillus nidulans”. In: *Journal of the American Chemical Society* 134.19 (Apr. 17, 2012), pp. 8212–8221. ISSN: 1520-5126. DOI: 10.1021/ja3016395.

[56] Nakazawa, Takehito et al. “Overexpressing Transcriptional Regulator in Aspergillus oryzae Activates a Silent Biosynthetic Pathway to Produce a Novel Polyketide”. In: *ChemBioChem* 13.6 (Mar. 2012), pp. 855–861. ISSN: 1439-7633. DOI: 10.1002/cbic.201200107.

[57] Chankhamjon, Pranatchareeya et al. “Regioselective Dichlorination of a non-activated Aliphatic Carbon Atom and Phenolic Bismethylation by a multifunctional fungal flavoenzyme”. In: *Angewandte Chemie International Edition* 55.39 (2016), pp. 11955–11959.

[58] Liu, Mengting et al. “AoiQ Catalyzes Geminal Dichlorination of 1,3-Diketone Natural Products”. In: *Journal of the American Chemical Society* 143.19 (May 6, 2021), pp. 7267–7271. ISSN: 1520-5126. DOI: 10.1021/jacs.1c02868.

[59] RT- PCR, A beginner’s guide to et al. “Beginner’s Guide”. In: (9173).

[60] Bong, Dajeong, Sohn, Jooyeon, and Lee, Seung-Jae V. “Brief guide to RT-qPCR”. In: *Molecules and Cells* 47.12 (Dec. 2024), p. 100141. ISSN: 1016-8478. DOI: 10.1016/j.mocell.2024.100141.

[61] Steiger, Matthias G., Mach, Robert L., and Mach-Aigner, Astrid R. “An accurate normalization strategy for RT-qPCR in Hypocrea jecorina (Trichoderma reesei)”. In: *Journal of Biotechnology* 145.1 (Jan. 2010), pp. 30–37. ISSN: 0168-1656. DOI: 10.1016/j.jbiotec.2009.10.012.

[62] Flatschacher, Daniel, Eschlböck, Alexander, and Zeilinger, Susanne. “Identification and evaluation of suitable reference genes for RT-qPCR analyses in Trichoderma atroviride under varying light conditions”. In: *Fungal Biology and Biotechnology* 10.1 (2023), p. 20.

[63] Punt, Peter J et al. “Transformation of Aspergillus based on the hygromycin B resistance marker from Escherichia coli”. In: *Gene* 56.1 (1987), pp. 117–124.

[64] Pfaffl, Michael. *A new mathematical model for relative quantification in real-time RT-PCR*. Tech. rep. Munich, 2001.

[65] Burger, Isabella et al. “In vivo activation of the dia BGC allows consolidation of the biosynthetic pathways of diaporthin, dichlorodiaporthin, diaporthinic acid, and diaporthinol”. In: *bioRxiv* (2025), pp. 2025–03.

[66] Li, Wensheng et al. “A New Antifungal Isocoumarin from The Endophytic Fungus Trichoderma Sp. 09 of Myoporum bontioides A. Gray”. In: (2016). DOI: 10.4103/0973-1296.192204.

[67] Larsen, Thomas Ostenfeld and Breinholt, Jens. “Dichlorodiaportin, Diaportinol, and Diaportinic Acid: Three Novel Isocoumarins fromPenicillium nalgiovense”. In: *Journal of Natural Products* 62.8 (July 1999), pp. 1182–1184. ISSN: 1520-6025. DOI: 10.1021/np990066b.

[68] Meng, Xiaolin et al. “Vital roles of Pks11, a highly reducing polyketide synthase, in fungal conidiation, antioxidant activity, conidial cell wall integrity, and UV tolerance of Beauveria bassiana”. In: *Journal of Invertebrate Pathology* 181 (Apr. 20, 2021), p. 107588. ISSN: 0022-2011. DOI: 10.1016/j.jip.2021.107588.

[69] Atanasova, Lea et al. “The polyketide synthase gene pks4 of Trichoderma reesei provides pigmentation and stress resistance”. In: *Eukaryotic cell* 12.11 (2013), pp. 1499–1508.

[70] Danner, Caroline et al. “Act1 out of Action: Identifying Reliable Reference Genes in Trichoderma reesei for Gene Expression Analysis”. In: *Journal of Fungi* 11.5 (2025), p. 396.

A. Appendix

Table A.1.: Utilized reagents and chemicals

Reagent	Manufacturer	Further information
Bacteriological Agar	VWR Chemicals BDH, Germany	Used for preparation of agar plates.
D(+)-Glucose Monohydrate for Biochemistry	Millipore ®, Sigma Aldrich Germany	
Malt Extract for Microbiology	Millipore ®, Sigma Aldrich Germany	
D-Sorbitol	Merck, Sigma Aldrich, Germany	
Polyethylene glycol 6000	Merck, Sigma Aldrich, Germany	
Sodium Chloride	VWR Chemicals BDH, Germany	
Uridine 99 % for Biochemistry	Carl Roth GmbH, Germany	
IGEPAL ® CA-630	Sigma Aldrich, Germany	
Glycerol 99.0 %	Merck, Sigma Aldrich, Germany	
Sodium Phosphate, Monobasic	Merck, Sigma Aldrich, Germany	
Sodium Dihydrogen Phosphate Monohydrate	Carl Roth GmbH, Germany	
Tween ® 80	Merck, Sigma Aldrich, Germany	
50x Tris-acetate-EDTA buffer (TAE-buffer)		The buffer was diluted and used as a running buffer to prepare agarose gels.

September 16, 2025

Reagent	Manufacturer	Further information
TopVision Agarose	Thermo Scientific™, Germany	For small gels, 0.4 g (to 50 mL TAE Bugger) Agarose was added, and for large ones, 0.96 g (to 120 mL TAE Buffer).
Midori ^{Green} Advance	NIPPON Genetics, Germany	DNA/RNA stain, used for staining the gel.
DNA Gel Loading Dye (6X)	Thermo Scientific™, Germany	Loading dye to make bands visible.
Quick-Load® Purple 1 kb Plus DNA Ladder	Thermo Scientific™, Germany	The range is between 0.1 to 10 kb.
5-Fluoroorotic Acid		
Vinotaste Pro	Novozymes, Bagsvaerd, Denmark	Enzyme Solution used for the extraction of protoplasts.

Table A.2.: Kits applied in this work

Kit Name	Manufacturer
Monarch® RNA Cleanup Kit (50 µg)	New England BioLabs®Inc.
Monarch® Plasmid Miniprep Kit	New England BioLabs®Inc.
Monarch® DNA Gel Extraction Kit	New England BioLabs®Inc.
LunaScript® RT SuperMix Kit	New England Biolabs ® Inc.
TriZol Zymo Reasearch Kit (Direct-zol™ RNA Miniprep Plus)	Zymo Reasearch

Table A.3.: RT-qpCR obtained raw data

Average Cts and Efficiencies									
Efficiency	**1,71**	**1,71**	**1,75**	**1,73**	**1,74**	**1,68**	**1,73**	**1,73**	**1,72**
Sample	**act1**	**sar1**	**Dia1**	**Dia2**	**Dia3**	**Dia4**	**DiaR1**	**DiaR2**	**TrAoiQ**
WT Average	22,1	19,6	28,6	26,7	23,3	27,0	26,7	28,0	24,8
QM6aI	21,5	19,1	28,7	28,5	23,1	27,2	26,7	27,3	24,0
QM6aII	22,2	19,8	28,6	26,7	23,7	26,9	26,7	27,8	25,0
QM6aIII	22,1	19,4	28,5	26,4	22,9	27,2	26,3	28,6	24,7
QM6aIV	22,1	19,7	28,6	27,0	23,2	26,9	27,1	27,6	24,6
OEI	21,9	19,4	24,4	24,3	21,2	23,5	18,2	25,1	23,0
OEII	23,1	20,4	26,6	27,2	23,4	25,6	18,9	27,3	23,1
OEIII	24,5	20,7	23,7	23,3	22,9	24,3	19,7	23,4	23,1
OEIV	23,6	20,8	24,4	24,8	22,5	22,9	19,3	25,3	21,9
819I	22,2	19,8	31,8	24,0	20,5	21,4	17,8	26,0	20,8
819II	22,4	19,5	27,7	24,2	21,4	22,4	17,6	25,3	21,6
819III	21,6	18,8	32,6	23,7	20,3	20,9	16,9	25,6	19,5
819IV	21,7	19,2	32,9	22,4	19,7	20,6	17,2	24,6	20,1
123I	19,6	19,0	16,7	17,6	30,0	14,3	18,4	19,1	15,9
123II	21,1	20,0	17,5	19,0	29,9	15,8	19,3	20,3	16,7
123III	20,4	19,3	17,3	17,9	31,2	15,2	18,6	19,6	16,7
123IV	23,5	22,4	20,0	21,1	27,4	18,1	20,8	21,8	19,2
25I	25,3	23,0	22,0	30,0	19,6	20,4	20,5	25,0	20,6
25II	24,7	22,3	22,2	31,6	19,5	20,3	20,0	24,9	20,6
25III	23,3	20,7	20,1	31,8	17,7	18,2	18,0	23,6	18,8
25IV	26,9	24,0	23,6	33,5	22,0	21,4	21,2	26,7	22,6
50I	24,2	22,6	22,4	23,5	20,0	27,4	19,7	26,3	22,0
50II	23,9	22,5	22,1	23,1	19,7	27,9	20,6	25,1	21,8
50III	25,4	23,5	22,6	24,2	20,4	28,5	21,1	26,3	22,8

Average Cts and Efficiencies									
50IV	25,2	23,2	24,5	26,1	22,3	27,7	20,2	27,9	24,5
52I	24,4	21,9	20,5	21,5	19,6	20,3	19,6	24,7	27,3
52II	26,5	23,4	21,9	22,5	20,5	21,2	21,1	26,0	27,6
52III	26,8	23,8	23,2	23,6	22,3	23,8	22,1	27,6	27,8
52IV	27,0	21,8	22,3	22,5	20,9	21,4	21,3	26,4	28,8

Table A.4.: Relative Transcript Abundance Levels for each strain in quadruplicates

Dia1	Dia2	DIa3	Dia4	DiaR1	DiaR2	TrAoiQ	
0,68	0,27	0,80	0,66	0,73	1,08	1,11	**QM6aI**
1,05	1,06	0,84	1,12	1,06	1,19	0,94	**QM6aII**
0,97	1,10	1,14	0,84	1,16	0,67	0,97	**QM6aIII**
0,99	0,86	1,05	1,06	0,81	1,26	1,10	**QM6aIV**
8,99	3,30	2,77	5,44	93,13	4,35	2,30	**OEI**
4,77	1,21	1,48	3,30	114,58	2,34	3,94	**OEII**
40,08	17,25	3,26	10,83	123,51	33,43	6,58	**OEIII**
20,71	5,77	3,11	17,11	117,33	8,97	9,63	**OEIV**
0,18	4,70	4,93	19,55	139,93	3,20	9,17	**819I**
1,69	4,12	2,93	11,38	152,83	4,60	5,81	**819II**
0,07	3,62	3,60	16,56	149,69	2,60	12,13	**819III**
0,07	8,42	5,71	22,05	144,73	5,14	9,98	**819IV**
360,49	72,01	0,01	356,12	45,84	64,75	59,63	**123I**
426,72	61,67	0,02	301,93	51,74	61,87	71,40	**123II**
327,79	77,57	0,01	283,38	52,18	62,48	49,06	**123III**
383,62	70,40	0,33	330,78	82,31	98,15	66,54	**123IV**
223,86	0,94	43,92	178,03	172,54	30,03	55,35	**25I**
141,19	0,28	32,73	132,22	160,01	22,37	39,03	**25II**
203,60	0,11	39,69	176,22	214,33	20,47	46,40	**25III**

Dia1	Dia2	DIa3	Dia4	DiaR1	DiaR2	TrAoiQ	
185,03	0,28	23,44	213,42	236,97	23,77	37,68	**25IV**
123,18	23,02	24,20	3,22	183,94	10,10	17,80	**50I**
132,64	26,13	26,03	2,26	102,33	17,81	18,08	**50II**
190,38	27,07	33,51	3,14	147,54	17,45	19,93	**50III**
57,54	8,30	10,19	4,15	210,49	6,31	6,90	**50IV**
301,67	58,71	25,66	109,56	165,10	20,69	0,85	**52I**
367,53	90,07	41,44	182,42	192,84	26,91	1,92	**52II**
214,04	59,13	18,38	56,77	133,94	13,41	2,07	**52III**
275,26	84,29	31,08	153,88	161,74	20,21	0,94	**52IV**
1419,16	306,10	212,52	142,17	37,59	0,49	154,56	**1121**
1422,76	493,90	166,74	106,16	99,36	0,71	224,18	**1122**
1256,14	164,26	132,56	73,14	39,15	2,66	105,76	**1123**

Relative transcript abundance (average)

Table A.5.: Relative Transcript Abundance Levels (Average of all Quadruplicates)

	dia1	*dia2*	*dia3*	*dia4*	*diaR1*	*diaR2*	*dia5*
QM6a (WT)	0,92	0,82	0,96	0,92	0,94	1,05	1,03
OEDiaR1	18,64	6,88	2,65	9,17	112,14	12,27	5,61
Δdia1	0,50	5,21	4,29	17,38	146,80	3,89	9,27
Δdia3	374,66	70,41	0,09	318,05	58,02	71,81	61,66
Δdia2	188,42	0,40	34,95	174,97	195,96	24,16	44,61
Δdia4	125,93	21,13	23,49	3,19	161,07	12,92	15,68
Δdia5	289,63	73,05	29,14	125,66	163,41	20,30	1,45

Relative transcript abundance (average)

Table A.6.: Calculated Standard Deviation for the Relative Transcript Abundance Levels (Average of all Quadruplicates)

	Dia1	Dia2	Dia3	Dia4	DiaR1	DiaR2	Dia5
QM6a	0,08	0,19	0,08	0,11	0,10	0,13	0,05
OE	7,90	3,58	0,40	3,08	6,61	7,19	1,60
819	0,40	1,09	0,63	2,30	2,83	0,59	1,31
123	20,79	3,29	0,08	16,00	8,23	8,80	4,84
25	17,63	0,37	4,47	16,63	17,93	2,07	4,06
50	27,21	4,36	4,87	0,39	23,45	2,83	2,96
52	31,80	8,24	4,86	27,42	12,04	2,76	0,32
Standard deviation/2							

Table A.7.: RT-qPCR Luna® Universal qPCR Master Mix Pipetting Scheme

Strain	**Value**
WT	0.292
OEdiaR1	0.32
dia1	0,191
dia2	0,2
dia3	0,049
dia4	0,157
dia5	0,131

PMT	Colonies counted	µg DNA used	CFU/µg
1	16	2	8,0
2	15	2	7,5
3	12	2	6,0

PMT	Colonies counted	µg DNA used	CFU/µg
4	16	2	8,0
5	12	2	6,0
Average			**7,1**

PMT	Colonies counted	µg DNA used	
1	26	5	5,2
2	28	5	5,6
3	24	5	4,8
4	24	5	4,8
5	31	5	6,2
Average			**5,3**

PMT	Colonies counted	µg DNA used	
1	26	7	3,7
2	37	7	5,3
3	33	7	4,7
4	29	7	4,1
5	33	7	4,7
Average			**4,5**

Chemical Transformation	Colonies counted	µg DNA used	Total volume after recovery µL	Volume plated µL	
1	13	10	2000	50	52
2	18	10	2000	50	72
3	16	10	2000	50	64
4	12	10	2000	50	48

PMT	Colonies counted	µg DNA used			CFU/µg
5	12	10	2000	50	48
Average					**56,8**